

The New Mexico Journal of Science

Natalie A. Rogers, Editor

THE NEW MEXICO ACADEMY OF SCIENCE



VOLUME 52
DECEMBER 2018

Table of Contents

Editor's Note	3
Junior Academy of Science 2018 Paper Competition Winners	4
<i>Modeling American Alligator Population Dynamics</i>	5
<i>Analyzing Patterns Within an Original Egyptian Fraction Decomposition Algorithm</i>	16
<i>Play "Spot The Difference" to Fight Cancer</i>	24
2018 Awards for Outstanding Science Teaching	33
New Mexico Academy of Science Research Symposium	34
About the Research Symposium	34
Keynote Speaker: Douglas Olson, PhD	34
Symposium Welcome from 2018 NMAS President	34
About the Sponsors	35
Concurrent Session Presentation Abstracts	36
Undergraduate Student Poster Abstracts	45
Graduate Student Poster Abstracts	52
Faculty Poster Abstracts	60
About the New Mexico Academy of Science	62
Contact Information	62
Officers and Executive Board 2018	62

Editor's Note

The *New Mexico Journal of Science* is a publication of the New Mexico Academy of Science. Each issue of the *Journal*, which has been published since 1906, contains research papers and articles deemed of interest to the scientists, educators, and citizens of New Mexico. Some volumes address scientific topics of social or economic interest to the state, while others emphasize scientific research in areas where New Mexico is particularly active.

The Academy oversees a New Mexico Junior Academy of Science program that sponsors an annual statewide scientific paper competition for students in New Mexico's high schools. This volume of the *Journal* contains the winners from that competition, as well as an additional paper.

The New Mexico Academy of Science Research Symposium was held in Albuquerque, New Mexico on October 28, 2018. Oral and poster presentations at the Symposium described scientific research conducted by undergraduate students, graduate students, and faculty at New Mexico's colleges and universities, and the abstracts of those presentations are once again included in this year's *Journal*. The New Mexico Academy of Science also presented its annual Outstanding Science Teacher Awards at the meeting. We wish to acknowledge the organizations which co-sponsored the 2018 Research Symposium: the New Mexico Experimental Program to Stimulate Competitive Research (NM EPSCoR), the Central New Mexico Local Section of the American Chemical Society (ACS), the New Mexico Alliance for Minority Participation (NM AMP) and the University of New Mexico (UNM) Center for Water and the Environment.

The *New Mexico Journal of Science* is published in an electronic-only format; it can be freely downloaded from the Academy's website at <http://www.nmas.org>. This enables the Academy to reach a much wider readership without incurring the considerable costs associated with the printing and distribution of paper copies.

Natalie A. Rogers, Editor
New Mexico Journal of Science

Public Relations Specialist
New Mexico EPSCoR
University of New Mexico
nrogers@epscor.unm.edu

New Mexico Junior Academy of Science 2018 Paper Competition Winners

Karin Ebey

Modeling American Alligator Populations Dynamics

Ana Mariá Pérez

Analyzing Patterns Within an Original Egyptian Fraction Decomposition Algorithm

Ksenia Sevostianov

Play "Spot the Difference" to Fight Cancer

Modeling American Alligator Population Dynamics

Karin Ebey, Los Alamos High School

ABSTRACT

The American alligator, *Alligator mississippiensis*, was hunted extensively until a management program was started in 1967. This management program, which is still used today, consists of hunting, egg collection, and farm release. The purpose of this experiment was to better understand the effects of human interaction and hurricanes on alligator population dynamics. The hypothesis was that human interaction can help the alligator population recover from hurricanes. A model was made using python code to test this. The model includes exponential growth, carrying capacity, aging, predator-prey interaction, hurricanes and human interaction in the form of farm release, egg collection and hunting. Without human interaction, the populations took three years to recover from a hurricane. Different variations of human interaction did not affect the recovery time. The hurricanes that occurred in Louisiana from 1950-2000 were modeled to determine if subsequent hurricanes affect recovery. The recovery was longer when hurricanes came in quick succession. Modeling a historical hunting level caused the alligator adult population to be very low. Managing the high historical hunting level with farm release and egg collection was attempted. No levels of farm release and egg collection manage this level of hunting, as increased farm release caused the alligator population to exceed the carrying capacity, which made it drop because there were not enough resources. The hypothesis was not supported because hurricane recovery was only minimally affected by human interaction. Successful management plans must balance alligator and human needs.

INTRODUCTION

The American alligator, *Alligator mississippiensis*, lives in the Southeastern United States. The American alligator was hunted extensively throughout the 1800 and 1900s until being put on the Endangered Species list in 1967. At that time, a management program was established to help the American alligator recover (Grigg & Kirshner, 2015). The program, which is still used today, consists of farmers collecting eggs, raising them, and releasing a percentage of the farm raised alligators back into the wild after they have matured. This program aids the population by ensuring more alligators make it past the juvenile stage where mortality is high. The program also includes hunting, with around 3% of the population available for hunting. This program has been highly successful in bringing back the alligator population (Louisiana Department of Wildlife and Fisheries (LDWF) 2016; Elsey 2017).

American alligator population dynamics need to be better understood because alligators are a valuable resource to the ecosystem and to the people living near them. As the apex predator at the top of the food chain, the American

alligator helps the ecosystem by keeping their prey from overpopulating, thus keeping the environment balanced (Grigg & Kirshner 2015). A large part of the management plan's success is that it makes the alligator valuable to the people living in regions with alligators, while maintaining the alligator population. In 2014 in Louisiana, 35,900 alligators were harvested in the hunting season, generating \$13.7 million, while 341,800 farm alligators were harvested, generating \$77 million. In addition, \$9.5 million worth of eggs were harvested through the management program. This comes to a \$100 million industry in Louisiana alone (LDWF 2016). This industry makes the alligator a valuable economic resource, so it is important the population remains stable, allowing harvesting to continue.

Alligator population dynamics are dependent on human interaction, natural disasters, and carrying capacity, which is the maximum population an area can sustain (Meyer 2016). The American alligator lives in a region prone to hurricanes, which occur about every three years. These natural disasters can significantly decrease

the population (Roth 2009). Hurricanes can occur in quick succession, like hurricanes Harvey and Irma in 2017, so understanding their impact on the alligator population is needed.

The goal of this experiment was to determine the effects of human interaction and hurricanes on American alligator population dynamics. It was hypothesized that human interaction can be used to keep the alligator population stable through hurricanes by hunting, egg collection and farm release.

METHODS

For this experiment, a computer model of American alligator population dynamics was created. A model is used because it allows exploration of different degrees of human interaction without testing in the real system. This is important because scientists do not have the luxury of being able to test this out in the real system after a hurricane because each hurricane is different and conditions are constantly changing, so the experiment cannot be repeated. A model also allows testing of the different methods without any risk to the population (Keen & Spain 1992). For this project, a model was created by writing a code using the Python 3.6.1. language. In the simulation time is measured in years.

In this model there are two species, the American alligator and a generic prey species. American alligators consume a wide variety of prey species over the course of their lives ranging from insects to deer to water fowl (Grigg & Kirshner 2015). A generic prey species, as opposed to many different prey species, is used to focus the effects of human interaction on the alligator population. The model begins by defining the variables used: G_a , G_y , and G_h , are the alligator adult (ages 2+),

alligator young (age 1) and alligator hatchling (age 0) populations, respectively. Likewise, P_a , P_y , and P_h are the prey adult (ages 2+), prey young (age 1) and prey hatchling (age 0) populations, respectively. The initial number of farm eggs, ef , is 0 because no eggs have yet been collected.

Table 1 shows the model initial conditions, including the starting populations and the values of carrying capacity and base mortality for each age group. Carrying capacity is the maximum population an area can sustain and base mortality is the percent of the population that survives each year and does not die off from natural causes like old age and disease (Meyer 2016). In the model the carrying capacity is higher for adults than young and hatchlings because the alligator population skews adult heavy (Grigg & Kirshner 2015). The carrying capacity for each prey population is several times higher than the carrying capacity of the respective alligator population as there are more prey in a system because they require fewer resources to sustain. The initial populations are based roughly on the carrying capacities for each age group. The base mortality is higher for hatchlings than for adults and young because hatchlings are smaller and more vulnerable to things like disease and flooding.

Next, years with hurricanes are defined. Hurricanes are assigned a category between one and five based on wind speed, with category five hurricanes being the most severe (Roth 2009). In this model, hurricanes are defined in two categories, with smaller hurricanes being in category 1-2 and larger hurricanes in category 3-5. Table 2 shows the model mortality coefficients for each hurricane category, where the coefficient is the percent that survives each hurricane, so in years without hurricanes, the hurricane mortality coefficient is 1 because 100% of the population

Table 1. The initial conditions in the model

Population	Initial Population	Age	Carrying Capacity	Base Mortality
Alligator Adults, G_a	250	2+	430	0.4
Alligator Young, G_y	250	1	290	0.4
Alligator Hatchling, G_h	250	0	250	0.2
Prey Adult, P_a	4300	2+	5630	0.6
Prey Young, P_y	2500	1	2860	0.4
Prey Hatchling, P_h	2500	0	2500	0.2
Farm Eggs, ef	0	NA	NA	NA

Table 2. The mortality coefficients due to hurricanes for the different age groups as a percent that survives the hurricane

Population	No Hurricane	Category 1-2	Category 3-5
<i>Ga</i>	1	1	0.5
<i>Gy</i>	1	0.6	0.3
<i>Gh</i>	1	0.5	0.1
<i>Pa</i>	1	1	0.5
<i>Py</i>	1	0.6	0.3
<i>Ph</i>	1	0.5	0.1

survives. The hurricanes that occurred in Louisiana 1950-2000 were identified with data from <http://www.wpc.ncep.noaa.gov/research/lahur.pdf> (Roth 2009).

Next, aging occurs, where hatchlings become young and young become adults. At this point, alligators raised on farms are released back into the wild into the alligator young population. The number released back into the wild is equal to the product of the farm release rate and the farm population. The number of alligator eggs and prey hatchlings is based on exponential growth, because populations grow exponentially unless growth is restricted (Keen & Spain 1992).

$$e = 0.3 * 25 * Ga * \left(1 - \left(\frac{Ga}{1000}\right)\right)$$

Equation 1. Alligator eggs (*e*)

$$Ph = 0.3 * 25 * Pa * \left(1 - \left(\frac{Pa}{10000}\right)\right) * 0.3$$

Equation 2. Prey hatchlings (*Ph*)

As shown in Equations 1 and 2, the number of alligator eggs and prey hatchlings is equal to the product of the percent of adults reproducing, 0.3, because half of the adults are male and not all adults are reproductively mature; the number of eggs per nest, 25 (Grigg & Kirshner 2015); the adult population, *Ga* or *Pa*; the carrying capacity ratio based on the adult population ($1 - (Ga/1000)$), because if there are many adults in the population then there will be fewer nests made because of competition for nesting space; and the percent of eggs that hatch, 0.3 for prey hatchlings.

$$ef = 0.2 * e$$

Equation 3. Farm eggs (*ef*)

$$Gh = 0.8 * 0.3 * e$$

Equation 4. Alligator hatchlings (*Gh*)

As shown in Equation 3, the number of alligator eggs taken to be raised on farms is a percentage of the total eggs.

As shown in Equation 4, the alligator hatchling population is equal to the product of the percentage of eggs left in the wild 0.8, the total number of eggs, *e*, and the percent of eggs that hatch, 0.3.

Equations 5 and 6 show examples of the methods used to model base mortality, carrying capacity, predator-prey interaction, hunting, and hurricanes. Each population model accounts for base mortality and carrying capacity. The populations are equal to the sum of the population and the product of the population, the base mortality rate (0.6 for *Pa*), and the ratio between the population and the carrying capacity subtracted from one ($1 - (Ga/430)$). Carrying capacity defines the total number of organisms the area can sustain. If the population exceeds the carrying capacity, it will decrease and if the population is less than the carrying capacity, it will increase because of immigration. Immigration occurs when individuals move from areas where the population exceeds the carrying capacity to areas where it does not, to get sufficient resources (Meyer, 2016). This is shown in the labeled parts of Equations 5 and 6.

Predator-prey effects are modeled based on interactions between the two species. For prey, the respective alligator population is subtracted from the population because of predation (Keen & Spain 1992), as shown in the labeled part of Equation 5. For alligators, the product of the number of alligators and prey, representing the number of times they cross paths, and the percent of times resulting in population growth is added to the population because when the prey population is high then the alligator population will increase because there is an abundance of food (Keen & Spain 1992). This is shown in the labeled part of Equation 6. Also, the percent of alligators hunted

$$Pa = Pab * \left(Pa + \left(0.6 * Pa * \left(1 - \left(\frac{Pa}{5630} \right) \right) \right) - Ga \right)$$

↑ Hurricane Coefficient
↑ Base Mortality
↑ Carrying Capacity
↑ Predation

Equation 5.

$$Ga = Gab * \left(Ga + \left(0.4 * Ga * \left(1 - \left(\frac{Ga}{430} \right) \right) \right) + (0.00001 * Ga * Pa) - 0.03 * Ga \right)$$

↑ Hurricane Coefficient
↑ Base Mortality
↑ Carrying Capacity
↑ Predator-Prey Interaction
↑ Hunting

Equation 6.

is subtracted from the population. This happens to the young and hatchling populations too, but only the adults are shown here. Finally, each population is multiplied by the appropriate hurricane mortality coefficient.

The populations for each year are then taken to be the number after all these interactions occur. To summarize: each year the population ages, the adults reproduce and then the populations decrease or increase because of predator-prey interaction, carrying capacity and hurricanes in applicable years.

The model was first run with no human interaction and no hurricanes to give a baseline for the alligator-prey interaction. Next, the model was run with no human interaction and an isolated hurricane to determine the effects of a single hurricane on the populations. Then the model was run adding human interaction in the form of egg collection, farm release and hunting with an isolated

hurricane. Finally, the model was run with human interaction and the hurricanes that occurred in Louisiana from 1950-2000 to find the effects of realistic hurricanes on the populations.

RESULTS

No Human Interaction

First the populations were modeled with no humans and no hurricanes to examine the populations under pristine conditions. As shown in Figure 1, the alligator and prey populations oscillated out of phase, with the magnitude of the oscillations decreasing over time. This validates the predator-prey interaction portion of the model because in the wild predator and prey populations oscillate out of phase with each other (Keen & Spain 1992). The young populations were one year off in their oscillations from the hatchling populations because when the

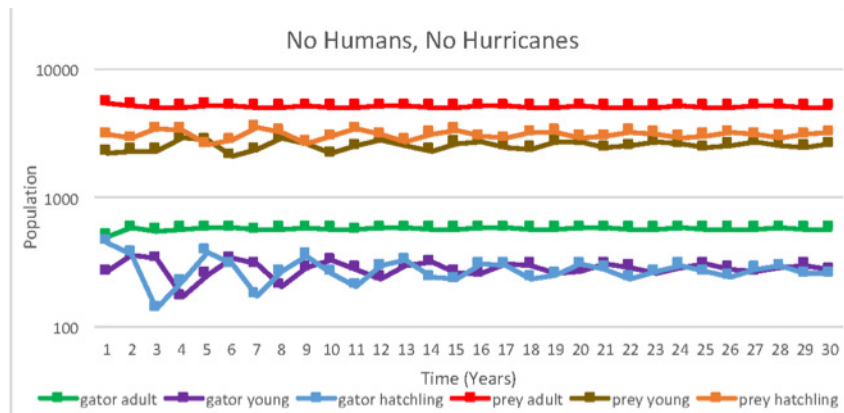


Figure 1. Population dynamics with no human interaction and no hurricanes. Population is plotted as a function of time in years. The alligator adults are plotted in green, young in purple, and hatchlings in blue, prey adults in red, young in brown, and hatchlings in orange. A logarithmic scale is used to show the relationships between the prey and alligator populations which are far apart.

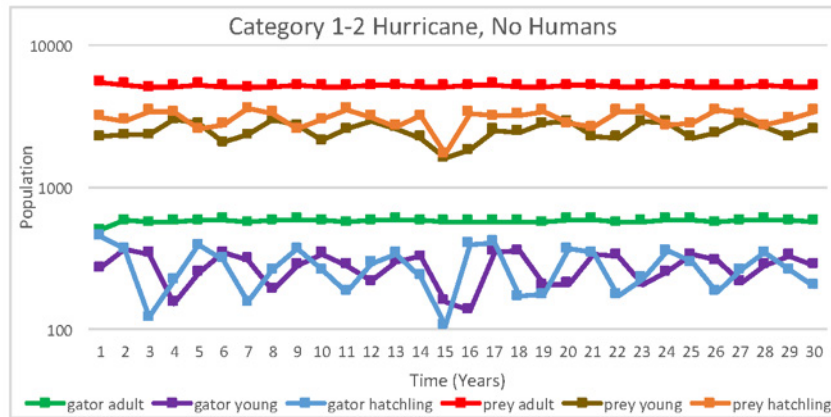


Figure 2. Population dynamics with no human interaction and a category 1-2 hurricane in year 15. Data are in the same format as Figure 1.

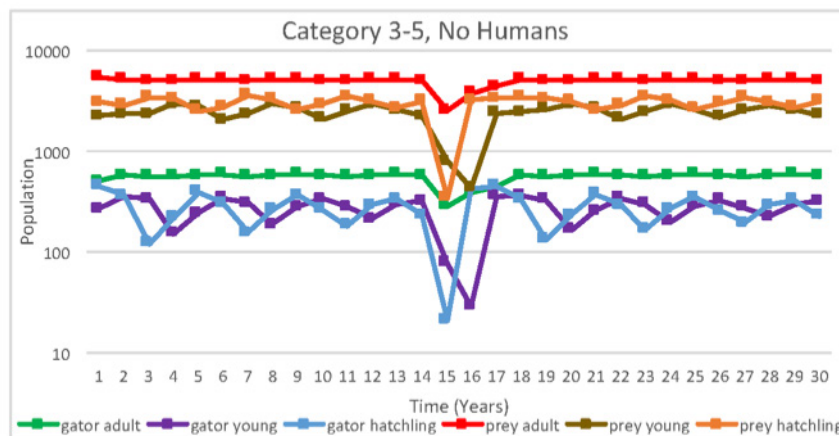


Figure 3. Population dynamics with no human interaction and with a category 3-5 hurricane in year 15. Data are in the same format as Figure 1.

hatchling population is high, then the following year the young population will be high. The adult populations did not oscillate.

Isolated Hurricanes

Populations were then modeled assuming a single isolated hurricane. Figure 2 shows the population dynamics with no humans and a single category 1-2 hurricane in year 15. After the category 1-2 hurricane, the hatchling populations took one year to recover and the young populations took two years to recover. The adults were not affected by the hurricane. After the hurricane the oscillations were large, like at the beginning of the simulation, and then again decreased with time. Figure 3 shows the population dynamics with no humans and a single category 3-5 hurricane in year 15. After the category 3-5 hurricane, the hatchling populations took one year to recover, the young populations took two years to recover, and the adult populations took three years to recover.

Figure 3 shows the population dynamics with no humans and a single category 3-5 hurricane in year 15. After the category 3-5 hurricane, the hatchling populations took one year to recover, the young populations took two years to recover, and the adult populations took three years to recover.

Human Interaction and Hurricane Recovery

Next, the effect of human interaction on recovery from an isolated hurricane was tested. Human interaction effects were tested starting from the management plan currently used in Louisiana: 20% Egg Collection, 12% Farm Release, and 3% and 1% hunting of alligator adults and young respectively (Elsley 2017). Category 1-2 hurricanes minimally impact the populations, and human interaction does not make an impact on the recovery so only category 3-5 hurricane results are shown here. For a category 3-5 hurricane, the population recovery using this management plan is shown in Figure 4. The

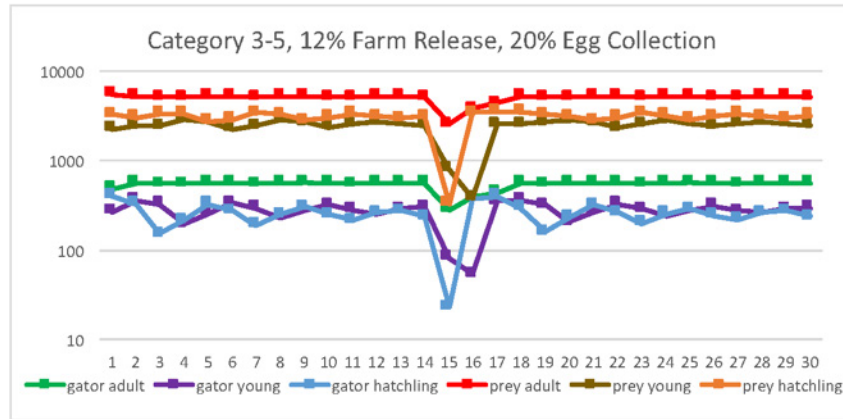


Figure 4. Population dynamics with 20% Egg Collection, 12% Farm Release, and 3% and 1% hunting of Alligator adults and young and a category 3-5 hurricane in year 15. Data are in the same format as Figure 1.

population recovery time was the same as the model with no human interaction, with slight differences in the exact values of the populations as seen by comparing the values in Figures 3 and 4.

The effect of varying the farm release rate was studied. The population recovery (not shown because the recovery is similar to the populations shown in Figure 4), was modeled with double farm release for two years after the hurricane and then with no farm release for two years after the hurricane, both with 20% egg collection. The alligator young population was slightly low (no release) or high (double release) in years 16, 17 and 18, directly after the hurricane, and the prey young population was slightly high (no release) or low (double release) in years 16, 17 and 18, but the recovery rates were the same. This shows that changes in the farm release rate do not significantly affect hurricane recovery. They affect the populations in the years directly after the hurricanes, but within five years after the hurricane the farm release method had no effects on the populations.

Variations in egg collection were also modeled. The population recovery, not shown, was modeled with 10% egg collection and 40% egg collection, both with 12% farm release. Compared to 20% egg collection, the alligator population overall was high (10% egg collection) or low (40% egg collection) and the prey population was overall low (10% egg collection) or high (40% egg collection). The alligator young population was low (10% egg collection) or high (40% egg collection) in the year directly after the hurricane. The recovery rates were the same. The egg collection rate does not affect the recovery after a hurricane. In the year after a hurricane, the alligator

Table 3. Hurricanes that occurred in Louisiana years 1950-2000

Year	Name	Category
1956	Flossy	2
1957	Audrey	4
1960	Ethel	1
1961	Carla	4
1964	Hilda	3
1965	Betsy	3
1969	Camille	5
1971	Edith	2
1974	Carmen	3
1977	Babe	1
1979	Bob	1
1985	Elena	3
1986	Bonnie	1
1988	Florence	1
1992	Andrew	3
1995	Opal	3
1997	Danny	1
1998	Georges	2

young population was slightly higher with a greater egg collection rate compared to a lower egg collection rate, but the populations recover in the same amount of time and the differences were very small, showing that egg collection did not significantly affect the hurricane recovery.

Louisiana Hurricanes

So far only isolated hurricane effects have been examined. To study the effects of back to back hurricanes, the

populations were modeled with the hurricanes that occurred in Louisiana 1950-2000, as shown in Table 3.

In this 50 year stretch of Louisiana history, 18 hurricanes occurred, with nine in category 1-2 and nine in category 3-5 (Roth 2009). Hurricanes occurred on average once every 2.5 years. The maximum number of years between hurricanes was six years between 1979 and 1985. Hurricanes occurred in consecutive years 5 times during this period. The populations were modeled with the hurricanes and 12% farm release, 20% egg collection, 3% and 1% hunting of alligator adults/young with results shown in Figure 5. The populations do not oscillate

because they are never stable for long enough, because of hurricanes continuing to hit. The recovery time was the same as with isolated hurricanes, except when hurricanes came within two years of each other; then the recovery time for each population reset when another hurricane occurred, so recovery was longer.

To study historical conditions, the populations were modeled with the hurricanes that occurred in Louisiana 1950-2000 with similar human interaction to what occurred at that time. Before year 19 (1969), in the simulation, the human interaction consists of no farm release or egg collection and a historical hunting rate of

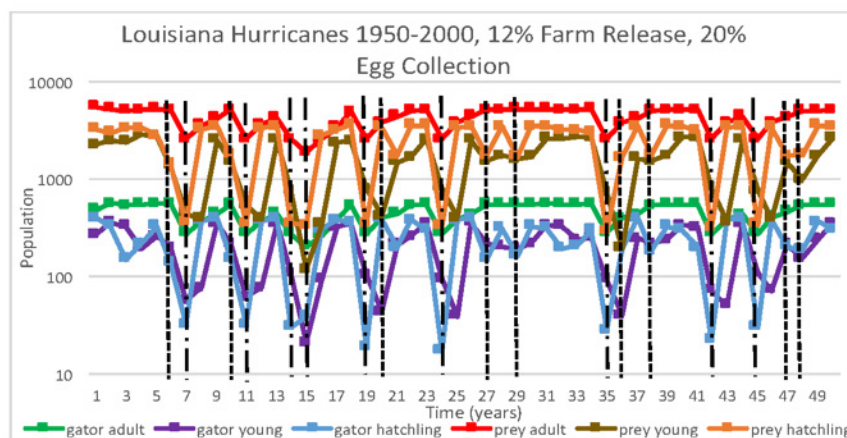


Figure 5. Population dynamics with 12% farm release, 20% egg collection and 3% and 1% hunting of alligator adults and young, with the hurricanes that occurred in Louisiana 1950-2000. Time is equal to years after 1950. Dashed lines indicate that a category 1-2 hurricane occurred in that year and dash-dot lines indicate that a category 3-5 hurricane occurred in that year. Data are in the same format as Figure 1.

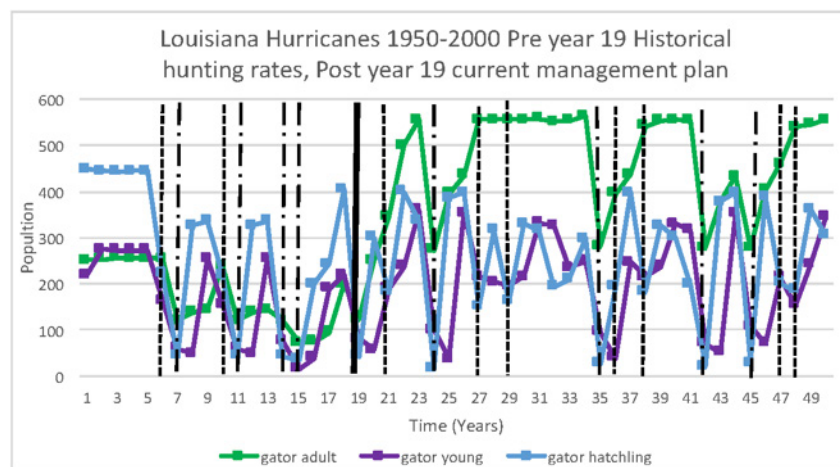


Figure 6. Population dynamics with the hurricanes that occurred in Louisiana 1950-2000. Before year 19, the human interaction consists of no farm release or egg collection and a historical hunting rate of 50% and 20% alligator adults/young. After year 19, the human interaction consists of the management program: 20% egg collection, 12% farm release, 3% and 1% hunting of alligator adults/young. The format is the same as Figure 5 except that it is on a linear scale because only the alligator populations are shown.

50% and 20% alligator adults/young. After year 19 the human interaction consists of the management program defined above. As shown in Figure 6, the alligator hatchling population was high before year 19 because all eggs are being left in the wild to hatch. The alligator young and adult populations were low before year 19 because of the heavy hunting level. After year 19 the populations returned to the level observed in the other simulations.

Next, the model was used to explore whether a historical hunting rate of 50% and 20% on alligator adults/young can be sustained through farm release and egg collection. The model was run with a historical hunting level and the 20% egg collection, 12% farm release levels from the management plan. As shown in Figure 7, the alligator hatchling population was higher than

the alligator adult and young populations because they are not affected by the high hunting level. The alligator young and adult populations were very low.

To see if an increased level of farm release and egg collection could balance this high level of hunting, the model was run with a historical hunting level and 50% egg collection, 25% farm release. As shown in Figure 8, the alligator hatchling population was about the same as the alligator adult and young populations because of the higher egg collection level. The alligator young and adult populations were still very low, showing that not enough alligators are being released into the system to balance the hunting level.

Since these levels of farm release and egg collection did not balance the hunting, an even higher level of farm

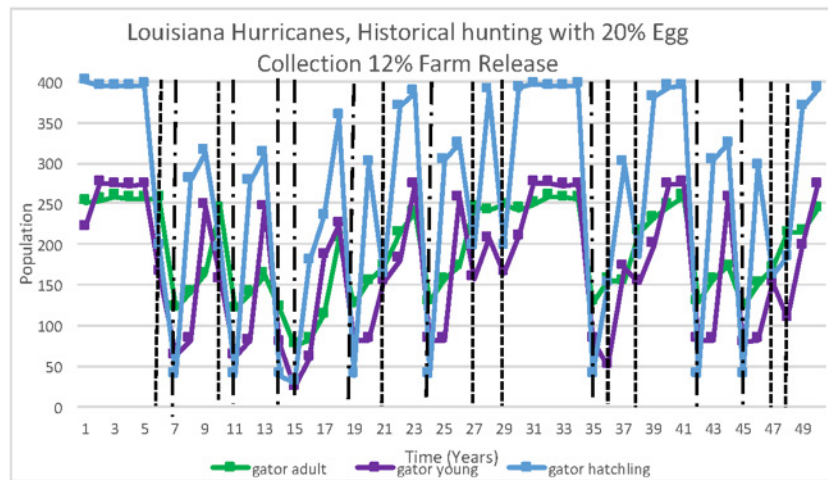


Figure 7. Population dynamics with the hurricanes that occurred in Louisiana 1950-2000, and a historical hunting level, 50% and 20% hunting of alligator adults/young, with 20% egg collection, 12% farm release, in the same format as Figure 6.

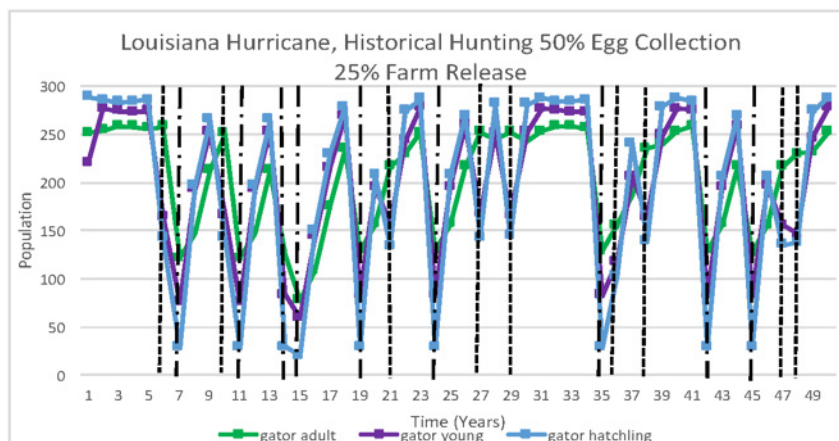


Figure 8. Population dynamics with the hurricanes that occurred in Louisiana 1950-2000, with a historical hunting level, 50% and 20% hunting of alligator adults/young, and 50% egg collection, 25% farm release, in the same format as Figure 6.

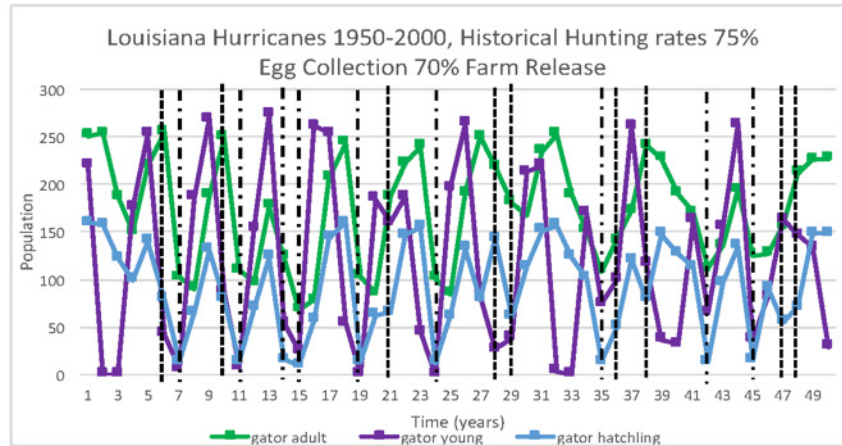


Figure 9. Population dynamics with the hurricanes that occurred in Louisiana 1950-2000, with a historical hunting level, 50% and 20% hunting of alligator adults/young, and 75% egg collection, 70% farm release, in the same format as Figure 6.

release and egg collection was modeled, with 75% egg collection, 70% farm release. As shown in Figure 9, the alligator hatchling population was much lower than the alligator adult and young populations because of the very high egg collection amount. The alligator adult population was still very low. The alligator young population fell to zero several times during the simulation. This is unexpected because farm release goes directly into the alligator young population. The reason it went to zero is that the amount being released significantly exceeded the carrying capacity, causing the population to drop to zero because of not enough resources.

These results show that a historical level of hunting cannot be sustained by egg collection and farm release because it is impossible to release the number of alligators necessary to compensate for the hunting level without exceeding the carrying capacity. These results show that high levels of egg collection and farm release can harm the populations, and so human interaction must be balanced to work.

DISCUSSION

Population Dynamics

The alligator young and hatchling populations oscillated out of phase with the prey young and hatchling populations. That is, the prey decreased when the alligator population increased and vice versa. This occurs because when the prey population is high, the alligator population will increase because there is an abundance of resources, thus causing the prey population to decrease

because many are consumed. A low prey population causes the alligator population to decrease because of not enough resources, thus allowing the prey population to increase. The young populations were one year off from the hatchling populations in the oscillations because the year after a high hatchling population, the young population is high. After a hurricane, the prey young and hatchling populations began at high level while the alligator young and hatchling populations decreased, and the oscillations began. The adult populations did not oscillate.

The alligator young population can be larger than the previous year's alligator hatchling population. This is due to farm release, if applicable, and carrying capacity. If the initial number of alligator young (the previous year's hatchling population) is low, then the population will increase because of growth through immigration, which is defined by carrying capacity. Immigration occurs when one area has an abundance of a species and another area does not, so individuals move to the less populated area. In contrast, the prey young population was usually smaller than the previous year's prey hatchling population because the amount of prey consumed in predation was greater than the amount added by immigration. In both the alligators and prey, the adult population was about twice the young population. This is because their base mortality is lower and they cover a larger age range, so the population is higher. This shows that environmental roles influence the population dynamics between different age groups.

Hurricane Recovery

The recovery of both species after a hurricane followed a pattern where the hatchling population was back to a normal population one year after the hurricane, the young two years, and the adults three years. The hatchlings took one year to recover because in the year after the hurricane there was no environmental pressure from the hurricane. Also, the adult population was lower, so there was less competition between the adults, helping the hatchling populations grow. The first year after a hurricane, the young population did not grow much because a small hatchling population from the year before filled their ranks, but they returned to normal the year after the hatchling population did. The adults took three years to recover, because they had to wait for a normal young population before they could return to normal.

The alligator recovery rate was based on the hatchling population returning to normal, and was not affected by any human interaction tested. All human interaction did was change how high the alligator young population was the year after the hurricane, while the year after that it was always back to normal because of the normal hatchling population.

CONCLUSIONS

The American alligator population dynamics were affected by the environment, prey, and human interaction. The prey caused the population to oscillate because when the prey population is high the alligator population increases and when the alligator population is high the prey population decreases. The environment contributed to growth and decay due to carrying capacity, deaths due to disease and old age, and natural disasters like hurricanes, from which the populations took several years to recover. Human interaction minimally affected the hurricane recovery.

The hypothesis was that human interaction can be used to keep the alligator population stable through hurricanes by hunting, egg collection and farm release. The hypothesis was not supported because the populations were stable without human interaction. Human interaction did not affect the recovery rate because the recovery was fueled by the hatchling population returning to normal the year after a hurricane, which outweighed the human interaction effects. Human interaction did make

the alligator populations closer to normal in the years directly after a category 3-5 hurricane with 40% egg collection, but did not change the recovery rate.

A historical level of hunting (50% on alligator adults, 20% on alligator young) was modeled to see if it could be managed by farm release and egg collection. This level of hunting was not manageable by farm release and egg collection because the adult population was fully reliant on the young population. The only way to increase the young population was through increased farm release, but with too much farm release the alligator young population exceeded the carrying capacity, so it dropped to zero. This is bad for the environment because it flushes the system with alligators that it cannot sustain, so the alligators die. This shows how too much farm release can be harmful to the populations.

Unregulated hunting caused the alligator population to be dangerously low, showing that human interaction can be harmful to maintaining the population stability. Without human interaction, the population would be fine, but that is unrealistic because alligators and humans live in the same areas. For human interaction to work, it must balance the number of alligators added to the population through farm release and the amount hunted. A management plan will only be successful if it both keeps the population stable over time and makes the alligator a valuable resource to the people.

Limitations and Future Directions

This model can be used to model population dynamics and recovery after natural disasters for other species of crocodilians. This is important especially for critically endangered species like the Gharial and Siamese Crocodile, which are likely to be lost if there is poor recovery after a natural disaster. A model allows scientists to try different recovery methods without risk of harming the population.

One limitation in this model is the fact that alligators consume many different species of prey at different times in their lives. Hatchling alligators eat primarily insects and small fish, while adults consume larger fish, birds and mammals. This model only includes one species of prey to focus on the effects of human interaction on American alligator population dynamics. In the future, this model should include different prey species for the different age groups. This addition would make the

model closer to what occurs in the system, increasing its accuracy.

Another improvement would be modeling the population over months, where predation and carrying capacity happen in all months and reproduction and hurricanes only happen in certain months. This would allow better understanding of season variations in the population dynamics and more educated planning as to when to hold hunting seasons.

This work demonstrates that more data on American Alligator population dynamics is needed. Models can only be validated by data from the system so with more knowledge, more realistic models can be made. A model is only as good as its limitations, so more data should be taken from the wild because with more knowledge, more accurate models can be made and more meaningful results can be obtained.

ACKNOWLEDGEMENTS

I thank Dr. Ruth Elsey for providing me with information on the Louisiana management program. I also thank my teachers Mrs. Thompson and Ms. Kline, and Ruth Skoug for assisting me in the editing process. I thank Ms. Tauxe for being my sponsor.

REFERENCES

“Alligator Program.” *Louisiana Department of Wildlife and Fisheries*, 2016, www.wlf.louisiana.gov/wildlife/alligator-program.

Grigg, G. and Kirshner, D. *Biology and Evolution of Crocodylians*. Cornell University Press, 2015, Ithaca, NY.

Elsey, R. 2017. Biologist Manager, Louisiana Department of Wildlife and Fisheries, Grand Chenier, LA. Personal communication.

Keen, R. and Spain, J. *Computer Simulation in Biology, A Basic Introduction*. Wiley-Liss, Inc, 1992, New York, NY.

Meyer, J. “Population Dynamics”. 2016. projects.ncsu.edu.

Roth, D. “Louisiana Hurricane History”. 2009. www.wpc.ncep.noaa.gov/research/lahur.pdf.

AUTHOR INFORMATION

Karin Ebey
Los Alamos High School
47gharials@gmail.com

Analyzing Patterns Within an Original Egyptian Fraction Decomposition Algorithm

AnaMaría Pérez, Albuquerque Academy

ABSTRACT

The exploration of Egyptian Fractions is part of the field of pure mathematics, Number Theory. First used by the Egyptians, they can be defined as proper fractions expressed through the sum of distinct unit fractions. Rather than having a method for decomposing fractions, the Egyptians used a chart. Eventually, the now-conventional greedy algorithm was applied to Egyptian fractions as a method for decomposition, but it is not necessarily the best. During the course of this project, a new algorithm was developed that tests have shown to be more efficient in some cases. But, whether or not the algorithm will always terminate has not been proven yet, but no cases contradicting termination have been found yet either. To take steps towards proving the functionality and termination of the algorithm, the sum lengths of multiple decompositions were analyzed for patterns and correlations that helped pinpoint sum lengths for various fractions. Based on these studies, it was found that the prime factorization of the denominator plus one was related to the lengths of these sums. Through analysis, significant steps toward achieving a proof of the new algorithm were taken and, in the process, more patterns within the algorithm were discovered.

INTRODUCTION

An Egyptian fraction can be defined as a fraction that is expressed as the sum of distinct unit fractions. Why distinct? The job of splitting a fraction into unit fractions is trivial when repeated fractions are allowed. $2/3$ would equal $1/3 + 1/3$, $3/4$ would equal $1/4 + 1/4 + 1/4$. But decomposing these fractions into unique and distinct fractions becomes more challenging to do. The Egyptians could only do this for fractions with 2 in the numerator and used a chart with pre-determined sums. Later, in order to address the problem of decomposing any fractions, a greedy algorithm was applied, meaning it takes the largest unit fraction out of the sum, then continues to take out increasingly smaller unit fractions until there is nothing left, giving it its name, greedy (Egyptian Fraction, 2017, Rhind, 2018).

During the course of this project, a different way of decomposing fractions was found, one that instead of testing fractions to find the biggest one that fits, uses a systematic process involving powers of 2 and a single equation. This algorithm, when tested against the conventional greedy algorithm, produced better sums in some cases: either less terms were involved, or denominators were smaller. In very special cases, the differences were very dramatic. But, though this algorithm works better, there is speculation that some cases may cause

a vicious cycle within the 4th step. In order to address this problem, a proof of the algorithm's functionality and termination was necessary, so over the course of this project, Perfect numbers, Mersenne numbers, and the sum lengths (the number of terms produced by the algorithm) were analyzed to try to prove the algorithm's termination. By proving it does, it will be possible to say with certainty that this algorithm does in fact work better than the greedy algorithm for the varying cases.

METHODS

In order to find patterns within the sum lengths to be able to predict them, data was gathered for a range of different fractions with various numerators and denominators. The denominators were all prime for the sake of ensuring no un-reduced fractions were present. The numerators that were tested in conjunction included numbers of the form 2^n , 2^{n-1} , and 2^{n+1} . This will provide a general idea of the decomposition of fractions with:

1. Numerators that expand to include a full set of powers of 2, meaning that in binary, the numerator would be written solely with 1s and no 0s;
2. Numerators with only a single power of 2 in the binary expansion; and
3. Numerators with a binary expansion of 2 numbers that sum to equal an odd number.

The sum lengths for each fraction were obtained through a computer program written in Scratch programming language (Scratch, 2018). Once data was gathered and recorded in Excel, the data was analyzed, and visual representations such as charts will be used to aid analysis. Using the data produced, equations were also found to explain the reasoning behind the sum lengths.

Algorithm

1. Split the numerator into the sum of powers of 2.
2. Divide both sides by the denominator.
3. Reduce and decompose* the non-unit fractions using this formula:

$$\frac{2^x}{d} = \frac{2^{x-1}}{(d+1)/2} + \frac{2^{x-1}}{d(d+1)/2}$$

Repeat step 3 until all numerators are equal to 1.

4. If necessary, combine like terms and repeat step 3. Repeat step 4 until all fractions are unit fractions, and all fractions are distinct.

RESULTS

Base 2 Relation

The formula used for the algorithm is based off of the decomposition for $2/d$ (Egyptian Fraction, 2017):

$$\frac{2}{d} = \frac{1}{(d+1)/2} + \frac{1}{d(d+1)/2}$$

And this formula can be used by extension for any number $2^x/d$:

$$\frac{2^x}{d} = \frac{2^{x-1}}{(d+1)/2} + \frac{2^{x-1}}{d(d+1)/2}$$

But, according to the algorithm, the numerator must first be decomposed into the sum of powers of 2.

Theorem 1: Every natural number can be written as the sum of distinct powers of two.

Ex. $57 = 111001$
 $1 \cdot 2^5 + 1 \cdot 2^4 + 1 \cdot 2^3 + 0 \cdot 2^2 + 0 \cdot 2^1 + 1 \cdot 2^0$

Table 1. Lemma 3

Numerator	Rule
2	$\frac{2}{d} = \frac{1}{(d+1)/2} + \frac{1}{d(d+1)/2}$
3	$\frac{3}{d} = \frac{2}{d} + \frac{1}{d}$
4	$\frac{4}{d} = \frac{2}{(d+1)/2} + \frac{2}{d(d+1)/2}$ Then either reduce or go to step 2 $\frac{4}{d} = \frac{1}{(d+3)/4} + \frac{1}{(d+1)(d+3)/8} + \frac{1}{(d^2+d+2)/4} + \frac{1}{d(d+1)(d^2+d+2)/8}$
5	$\frac{5}{d} = \frac{4}{d} + \frac{1}{d}$
6	$\frac{6}{d} = \frac{4}{d} + \frac{2}{d}$
7	$\frac{7}{d} = \frac{4}{d} + \frac{2}{d} + \frac{1}{d}$

*:This algorithm has not been proven to always work, but in all tested cases it does, and it has been proven to work for any case with a Mersenne prime in the denominator, all cases involving a 3 in the numerator, and in most fractions with a prime denominator.

This is proved through induction reasoning (Introduction to Abstract Mathematics, 1997).

Conjecture 2: All fractions can be expressed using a series of equations.

Lemma 3: Fractions $3/d$ will have a sum length of 3 given that d is an odd integer and is not divisible by 3.

This is shown by Table 1 since fractions $3/d$ can be expressed through these formulas. If d is divisible by 3, then the sum length will be 1, because it would reduce with the numerator. If d is even, then the sum length will be 2 because when 3 is broken into $2/d + 1/d$, the denominator, yet again, will reduce with the numerator. Additionally, the decompositions formulas for denominators 2-7 can be found in Table 1.

Perfect Number Relation

Because Perfect numbers so far have been the numbers found to require the use of step 4 of the algorithm the most, it is first necessary to examine how they work, and why they require the use of step 4. It is also necessary to see how they decompose.

Definition 4: A positive integer that is equal to the sum of its proper positive divisors, that is, the sum of its positive divisors excluding the number itself (Wells, 1997, Perfect Number, 2018).

Theorem 5: An even positive integer is a perfect number, that is, equals the sum of its proper divisors, if and only if it has the form $2^{p-1}M_p$ where M_p is a Mersenne prime (i.e. a prime number of the form $M_p = 2^p - 1$) (Perfect Number, 2018).

Euclid's Formation Rule (IX.36): $q(q+1)/2$ is an even perfect number whenever q is a prime of the form $2^p - 1$ for prime p (Perfect Number, 2018).

Since the binary sum of the original fraction is written out with only powers of 2 in the numerator, they will reduce with the 2^{p-1} component of the perfect number, leaving the Mersenne prime component in the denominator. Since the second fraction of the decomposed equation

$$\frac{2^x}{d} = \frac{2^{x-1}}{(d+1)/2} + \frac{2^{x-1}}{d(d+1)/2}$$

is of the form $q(q+1)/2$ as mentioned in Euclid's Formation Rule (IX.36), and the reduced denominator is of the

form $2^p - 1$, then the new set of fraction denominators produced by this formula are a Mersenne prime (d), the corresponding power of 2 that when multiplied by the Mersenne prime produces a perfect number $((d+1)/2)$, and the correlating perfect number $(d(d+1)/2)$.

$$\begin{aligned} \frac{2^x}{d} &= \frac{2^{x-1}}{(d+1)/2} + \frac{2^{x-1}}{d(d+1)/2} \\ \frac{2^x}{(2^n-1)} &= \frac{2^{x-1}}{((2^n-1)+1)/2} + \frac{2^{x-1}}{(2^n-1)((2^n-1)+1)/2} \\ \frac{2^x}{(2^n-1)} &= \frac{2^{x-1}}{2^{n-1}} + \frac{2^{x-1}}{(2^n-1)(2^{n-1})} \\ \frac{2^x}{(2^n-1)} &= \frac{1}{2^{n-x}} + \frac{1}{(2^n-1)(2^{n-x})} \end{aligned}$$

This property of perfect numbers allows for the simple reduction of any fraction with a perfect number in the denominator, due to the repetition of this cycle of decomposition.

Mersenne Number/Geometric Sequence Relation

Definition 6: Mersenne numbers are numbers of the form $M_n = 2^n - 1$ for some integer n (Mersenne Prime, 2018).

Definition 7: A Mersenne prime is prime number that can be written in the form $M_n = 2^p - 1$ for some integer p (Mersenne Prime, 2018).

Lemma 8: For any fraction $(2^n - 1)/(2^p - 1)$ where $2^p - 1$ is prime, the sum length will exactly equal $2^n - 1$.

Due to the same principles as perfect numbers, the decompositions are concise. The length is predictable because when broken down into the sum of powers of 2, each fraction splits into 2 separate unit fractions, except for the last fraction which is already in unit fraction form.

$$\begin{aligned} \frac{2^n - 1}{(2^p - 1)} &= \frac{2^{n-1}}{(2^p - 1)} + \frac{2^{n-2}}{(2^p - 1)} + \dots + \frac{2^{n-n}}{(2^p - 1)} \\ &= \left(\frac{1}{2^{p-n+1}} + \frac{1}{2^{p-n+1}(2^p - 1)} \right) \\ &\quad + \left(\frac{1}{2^{p-n+2}} + \frac{1}{2^{p-n+2}(2^p - 1)} \right) \\ &\quad + \dots + \left(\frac{1}{2^{p-n+n}} + \frac{1}{2^{p-n+n}(2^p - 1)} \right) \end{aligned}$$

In this case, the last unit fraction has been split up into 2 additional unit fractions, which can then be added to produce a separate unit fraction with the original denominator, simplifying the sum in both length and complexity

These fraction sums can also be expressed using reverse geometric sums (typically, geometric sums start with terms and arrive at a sum, but on the contrary, here, the sum is known, but not the terms). Mersenne numbers can be expressed as a partial geometric sum, implying they are the sum of consecutive powers of 2:

$$\sum_{k=0}^{n-1} 2^k = 2^n - 1$$

By extension, when Mersenne numbers are in the numerator, and Mersenne primes in the denominator, fractions can be expressed in this way:

$$\frac{2^n - 1}{(2^p - 1)} = \sum_{k=1}^n \left(\frac{1}{(2^{p-n+k})} + \frac{1}{(2^{p-n+k})(2^p - 1)} \right)$$

Similar to the fraction sums, the sum length when using geometric sums is $2n$ rather than $2n-1$, but in order to achieve the smaller sum, the last 2 fractions must be added to produce the unit fraction with the original denominator. There is speculation the it would work with Mersenne Numbers in the denominator as well, but due to limitations, especially when reducing, primes are easiest to use because they do not reduce being that they are only divisible by one and itself.

Lemma 9: Any number n can be expressed as a sum of powers of 2 when subtracted from the power of 2 larger than n .

The difference of the power of 2 and n can be expressed as the sum of powers of 2 due to Theorem 1.

Lemma 10: For any even numerator over a Mersenne Prime denominator, if the numerator is converted to binary, then the digits are added to produce q , then the resulting sum length is equal to $2q$. For any odd numerator, the resulting sum length is $2q-1$.

Due to this property of geometric sums, the length of any fraction with a Mersenne Prime in the denominator is predictable because of Lemma 6. When the power of 2 greater than the numerator is divided by the denominator,

it can be expanded to form a reverse geometric sum, and then, various pairs of fractions can be subtracted out in accordance to the powers of subtracted from the larger power of 2 to obtain n .

Exploration of Predictable Sum Lengths with Prime Denominators

Conjecture 11: The sum length of a given fraction with a Mersenne Number numerator and a prime denominator will correlate to the mod 8 division of the denominator and be predictable in relation to its mod 8 form.

After analysis of all the primes less than 2000, and the correlating sum lengths, it appears that there are no set sum lengths, at least based on mod 8. But it appears that the closer to a power of 2 that a denominator is, the more predictable. The resulting data produces a graph that resembles a tree. At each Mersenne number, the number of possible sum lengths increases. Even though the final length is not yet predictable, up to about denominator 63, there appear to be distinct tree lines. The greater sum lengths, displayed in pink, are the result of prime denominators that can be represented as 1 mod 8, and when the highest points for each numerator were analyzed, it was found the binary form of the denominator was always contained a minimal amount of 1s, either 2 or 3, suggesting less terms in the original binary expansion of the fraction. The lower sum lengths here deal with prime denominators that can be represented as 7 mod 8. Here appeared more 1s in the binary form of the number, suggesting more terms in the original binary expansion.

Chart Explanation (figure 1): Each line on the chart represents a different prime denominator, and each color represents the prime number in mod 8. The lighter the shade of color, the smaller the number is. On the x axis are the correlating numerators that combined with the various prime denominators. Each of these numerators is a Mersenne Number.

Listed using the y axis is the sum length of the decomposition, or the number of terms in the sum when decomposed. Both use log scales. Since the relation to mod 8 did show correlation, but was still unpredictable, a more general correlation was sought after. After further examination of these patterns, different correlations were found that better explained the data from the original testing.

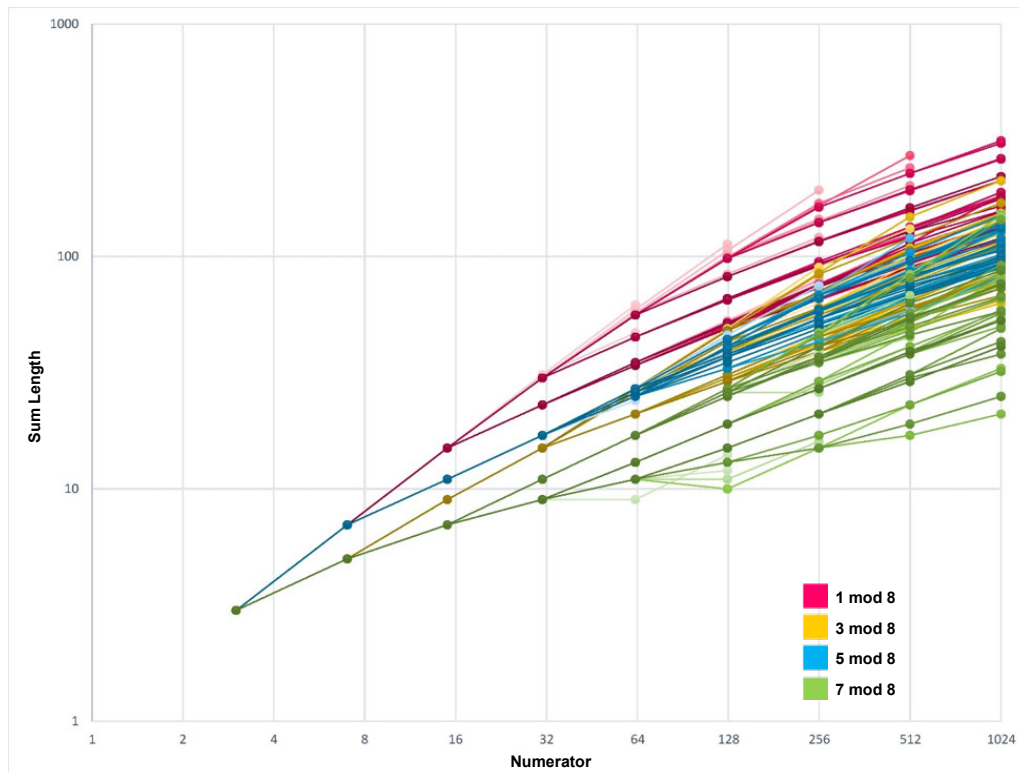


Figure 1. Model of Conjecture 11.

Lemma 12: The sum length will correlate to the prime factorizations of $(d+1)$.

While the theory about mods was not completely off, it did not incorporate all the aspects that could be addressed. Instead, by looking at the prime factorization of $(d+1)$, it takes into account the possibility of more 2's in the prime factorization. Using mod 8 did something similar, because numbers for example that were $3 \pmod{8}$, when 1 is added to them, have a prime factorization of $22 \cdot k$ with k being an odd number. Numbers that are $7 \pmod{8}$, when 1 is added to them, have a prime factorization of $23 \cdot k$. This said, since in Figure 1 it is apparent that fractions with a denominator that is $7 \pmod{8}$ are the lowest, and $3 \pmod{8}$ coming next in line, it can be observed that the sum length is most strongly correlated to the prime factorization of the denominator added with 1.

The number of factors that are 2 will dictate how well it decomposes with the derived formula. The formula decomposes each fraction into two more fractions, with new denominators $(d+1)/2$ and $d(d+1)/2$. This would explain why the number of powers of 2 in the prime factorization of $(d+1)$ would come into effect. The more powers of 2, the further the denominator can be

simplified in relation to the numerator, and when the fraction is able to be simplified, then the formula will have to be applied less times, meaning less fractions will be produced over all.

Conjecture 13: The sum length for a numerator n will be equal to the sum of the lengths for the corresponding fraction decompositions for the powers of 2 that sum to equal n .

This hypothesis was tested between 3 sets of data: the data with the sum lengths corresponding to each power of 2 in the numerator; the data with $2^n - 1$ in the numerator; and the data with $2^n + 1$ in the numerator. When the data for $2^n + 1$ in the numerator was compared against the data for 2^n in the numerator, no cases showed it to go against this hypothesis. On the other hand, a few cases for the data with $2^n - 1$ in the numerator prove it to be incorrect. An explanation for this can be found in step 4 of the algorithm, dictating that any fractions that share a denominator should be recombined, and re-reduced. When the denominator of these two fractions is even, then the decomposition will be shorter by one fraction because they were added and reduced. Of the 2259 fractions tested, on 29 of them, or 1.284% of them were not equal to the sum of the sum lengths for the fractions

with 2^n in the numerator. This would imply that the majority of fractions with prime denominators do not require step 4.

For the numbers that do not follow conjecture 13, there is a strong possibility that these denominators all have something in common that would allow them to have fractions that can combine. For example, non-prime denominators that often require fractions to be combined and simplified are perfect number denominators. As explained above, their factors allow them to be combined and simplified several times. These denominators that allow for combination may be similar, but as of now, no correlation can be found between them. Once a correlation is found, whether or not the cycle of combining fractions will end can be further determined, taking an even greater step in the proof of this algorithm.

By showing that so many of the fractions do not deal with the cycle of combining like terms, it is definite for these fractions that the algorithm will always terminate. In Table 1, it can be seen that fractions with 2^n in the numerator have set equations for their decomposition with sum lengths of 2^n . These equations are determined by imputing the expression for the denominator that is to be decomposed in place of the variable d in the following step:

$$\frac{2^n}{d} = \frac{2^{n-1}}{(d+1)/2} + \frac{2^{n-1}}{d(d+1)/2}$$

$$d_1 = \frac{d+1}{2} \quad | \quad d_2 = \frac{d(d+1)}{2}$$

$$\frac{2^n}{d} = \frac{2^{n-2}}{(d_1+1)/2} + \frac{2^{n-2}}{d_1(d_1+1)/2}$$

$$+ \frac{2^{n-2}}{(d_2+1)/2} + \frac{2^{n-2}}{d_2(d_2+1)/2}$$

Again, referencing Table 1, in some cases these fractions will reduce if the denominator's $(d+1)$ prime factorization contains 2^n with $n > 1$. This explains the inconsistency between various numbers in the data for fractions with 2^n in the numerator.

Lemma 14: Fractions with a power of 2 in the numerator

when decomposed will not produce any equal fractions.

For the fractions to be equal, after decomposition they must have the same denominator, and for this to happen:

$$d = \frac{d+1}{2} \quad \text{or} \quad \frac{d(d+1)}{2}$$

d would have to equal 1 for this to work, which would make the "fraction" into simply an integer. Extending to further equations as the power of 2 in the numerator grows,

$$d_1 = \frac{d_1+1}{2} \quad \text{or} \quad \frac{d_1(d_1+1)}{2}$$

Meaning d_1 would have to be equal to one, and since

$$d_1 = \frac{d+1}{2} \quad \text{therefore} \quad 1 = \frac{d+1}{2}$$

d must still be equal to one. The same applies for fractions of the d_2 track.

Chart Explanation (figure 2): Each line on the chart represents a different prime denominator. On the x axis are the correlating numerators that combined with the various prime denominators. Each of these numerators is a power of 2. Listed using the y axis is the sum length of the decomposition, or the number of terms in the sum when decomposed. Both axis use log scales.

This graph, like figure 1, also resembles a tree, with more varying data in the center, and the edges cleaner. But, more importantly, in the data, when there are straight lines between 2 points, that signifies that the denominators at that point could all be reduced by a factor of 2 in the next step, meaning none of them decomposed. Additionally, it can be observed that disregarding straight lines, the data tends to grow exponentially. With the knowledge of the divisibility of the denominator plus one, these flat lines can be determined, along with other instances of reduction.

CONCLUSIONS

Overall, through this study, an algorithm was found that allows for the decomposition of any fraction, in theory. While it has not been proven to work in any case, there

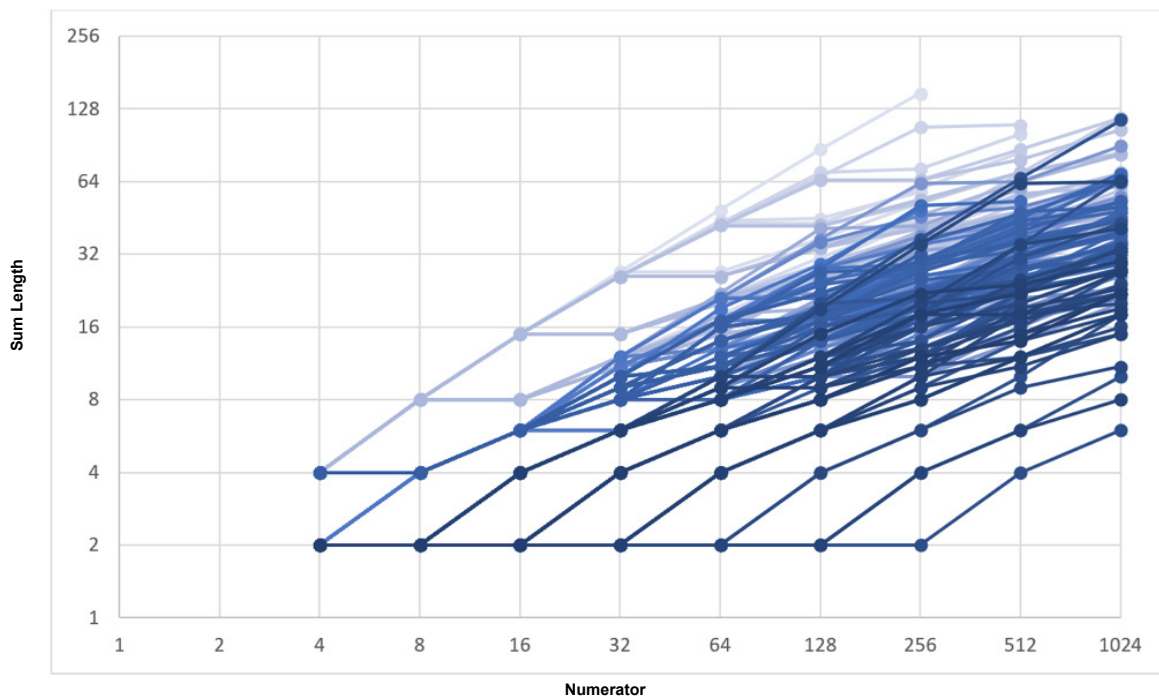


Figure 2. Model of Conjecture 13.

are no cases against this, and various Lemmas were found proving many cases are always decomposable. The cases left to prove whether or not termination of the algorithm will occur are those that do not agree with *Conjecture 13*. Through further research, correlations between these denominators and the reason for their combining of denominators may be found, providing the final piece to the puzzle regarding the proof of the termination of the algorithm. While only prime denominators were tested during this study, patterns found do not seem only applicable to primes, signifying that these results would apply to other odd numbers, and also even numbers, but in a slightly different way, seeing as they would be reduced first before continuing the process.

In further research, I would like to explore the fractions that did not follow *Conjecture 13*, and their relations to perfect numbers. Perfect numbers are the numbers that were found to require the use of step 4 of the algorithm the most, and this was discovered to be because of their prime factorization and the fact that a Mersenne number was involved. Similarly, I think these fraction that require the use of step 4, with further exploration,

will be able to be predicted based on their properties involving the prime factorization of $(d+1)$. Additionally, though a generalization was found for the sum lengths of fractions with a power of 2 in the numerator, noting it also had to do with the prime factorization of $(d+1)$, it may be possible for a method to be found to find more exact values for the sum lengths of these fractions. By further researching these different areas, a more conclusive proof can be found. Additionally, it is possible that the findings of this research could be applied to calculus. One technique of integration commonly used to solve integrals is dividing the function into a set of partial fractions. With further research in this specific area, it would be possible to find how these findings can be applied.

ACKNOWLEDGEMENTS

Special thanks to Dr. Vassilev of UNM, who helped me to present this research in a more professional format for a math paper. Thank you to my sponsor Mr. Fowler and my math teacher Dr. Vraspir, too, for helping read my abstract for clarity and conciseness.

REFERENCES

- “Egyptian Fraction.” *Wikipedia*, 2017, wikipedia.org/wiki/Egyptian_fraction.
- “Egyptian Fraction.” *Math World*, Wolfram Web Resources, 2018, mathworld.wolfram.com/EgyptianFraction.html.
- Eves, Howard. *An Introduction to the History of Mathematics*. Saunders College, 1990, Philadelphia, PA.
- “Introduction to Abstract Mathematics.” *Distinct Powers*, Salisbury University, 1997, faculty.salisbury.edu/~km-shannon/math300/distinctpowers.pdf.
- “List of Perfect Numbers.” *Wikipedia*, 2018, wikipedia.org/wiki/List_of_perfect_numbers.
- “Mersenne Prime.” *Wikipedia*, 2018, wikipedia.org/wiki/Mersenne_prime.
- “MIT Media Lab.” *Scratch*, Lifelong Kindergarten Group, 2018, scratch.mit.edu.
- “Perfect Number.” *Wikipedia*, 2018, wikipedia.org/wiki/Perfect_number.
- “Rhind Mathematical Papyrus 2/n Table.” *Wikipedia*, 2018, wikipedia.org/wiki/Rhind_Mathematical_Papyrus_2/n_table.
- Struik, Dirk J. *A Concise History of Mathematics*. 1987, Dover, NY.
- Wells, D. G. *The Penguin Dictionary of Curious and Interesting Numbers*. Penguin Publishing, 1997, London, England.

AUTHOR INFORMATION

AnaMaría Pérez
Albuquerque Academy
pera200@aa.edu

Play "Spot The Difference" to Fight Cancer

Ksenia Sevostianov, Sierra Middle School

ABSTRACT

Bone cancer results in an increased concentration of proteins called alkaline phosphatase (ALP). Since their concentration is higher in cancer cells, we can say that their function is more important for cancer cells than for healthy ones. For this reason, any inhibitor of alkaline phosphatase is expected to create chaos in the cancer cells and stop their growth. Recently, many possible inhibitors for ALP have been found. The main concern, however, remains unanswered: can these inhibitors interact with other phosphatases in cells and destroy healthy cells instead of sick ones? Wouldn't it be that the effect of "drugs" is worse than the disease itself? To answer this question, in this project we tested the inhibitory activity of the possible inhibitors toward ten different phosphatases including ALP. First, Chimera software and freely available databases RCSB and UniProt were used to study structures of several phosphatases and identify their important features such as sequences of amino acids near the active sites of the proteins, shapes and location of the active site pockets. Then, using freely available Avogadro software, structures of twenty five potential inhibitors were built. Their interactions with ALP (PDB code:1B8J) and other phosphatases was modeled using freely available docking software AutoDock Vina through RPBS Mobyle Portal web service. The inhibitors that were able to interact with ALP to slow down/stop its activity and did not interact with other phosphatases were identified.

INTRODUCTION

Bone cancer

This project is dedicated to finding a potential drug for bone cancer. Cancer affects millions of people all over the world every year. The original cancer tumor is known as "primary tumor". When cancer cells from the primary tumor spread to other organs and form a new tumor in a new place, it is known as "secondary cancer" or metastasis. There are many different types of cancer, but one of the most painful ones is bone cancer. Primary bone cancer is cancer that starts in the bones, while cancer that started in some other organ and then spread to the bones is called "secondary bone cancer" or "metastatic bone cancer". The chance of recovery for primary

bone cancer has improved in recent years because of new and better treatments, but it is still very low. This year, an estimated 3,260 people of all ages (1,820 men and boys and 1,440 women and girls) in the United States will be diagnosed with primary bone cancer, and 1,550 deaths (890 men and boys and 660 women and girls) will result from this disease (Figure 1).¹

The University of Rochester Medical Center states² that for all bone cancers combined, the 5-year survival rate (percent of people who live at least 5 years after the cancer is found) is about 70%. This varies by cancer type and stage. For osteosarcomas and Ewing sarcomas that are still in the area where they started (localized), the 5-year survival rate is about 60 to 80%. If the cancer has

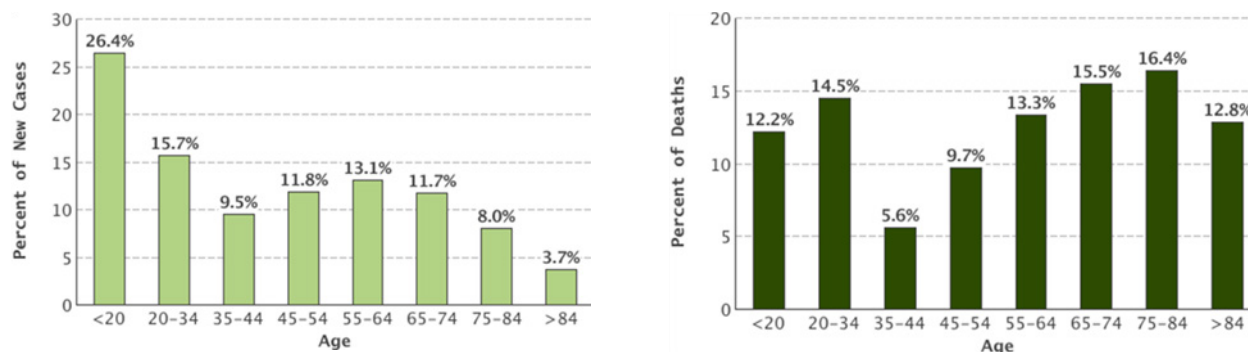


Figure 1. The percent of new cases of bone cancer diagnostics (left) and percent of deaths (right) at different ages as of 2018.

spread to other parts of the body, the 5-year survival rate is about 15 to 30%.

However, less than 0.2% of all cancers are primary bone cancer, and it is much more common for bones to be a site of metastasis or spread from other cancers. Once the cancer invades the bones, the prognosis is generally very poor. Advanced secondary bone cancer treatment generally includes palliative treatment which is focused on reducing the symptoms. Since it is hard to remove cancer in advanced stage, the survival rate is very low. Patient who receive the proper treatment and therapy (if metastasis in bones is detected early) may survive only for 2-3 years. The life expectancy of a patient depends mainly on the overall health (physical and mental) of the patient, the type of primary cancer, stage of the disease, and how aggressive the cancer cells are. Finding the drugs for secondary bone cancer treatment is one of the most important problems in biochemistry.

Alkaline Phosphatase

Presently, there is a lot of evidence that bone cancer (osteoblastic bone tumor) is accompanied by a high level of alkaline phosphatase.³ Alkaline phosphatase (ALP) is an enzyme that releases the phosphate under alkaline conditions and is made in liver, bone, and other tissues. A test to check the level of alkaline phosphatase is one of the standard tests in cancer diagnosis. The increased level of ALP in cancer cells probably means that this protein is very important for cancer cells. Therefore, blocking the biochemical activity of alkaline phosphatase will potentially lead to cancer cells not thriving.

Drug Development Strategy

Finding drugs for cancer treatment is one of the biggest and most challenging scientific problems today. The drug discovery strategy consists of several steps. First, it is important to identify the protein (enzyme) associated with cancer. Enzymes are biological molecules that act as catalysts to speed up chemical reactions in the living organisms. Without the presence of enzymes, these chemical reactions would progress too slowly.⁴ In 1894, Emil Fischer introduced the lock-and-key model to explain the exact action of an enzyme with a single substrate.

According to the “lock and key” model, an enzyme's active site has a specific shape, and only a specific

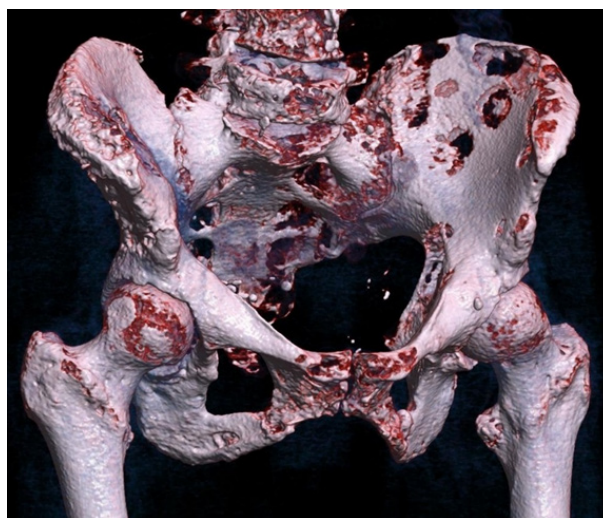


Figure 2. 3D computer tomography scan of bone metastases of the hip bone, in a 60 year old woman (Creative Commons Public Domain).



Figure 3. Crystalline structure of alkaline phosphatase (PDB code: 1B8J; image generated by PyMOL).

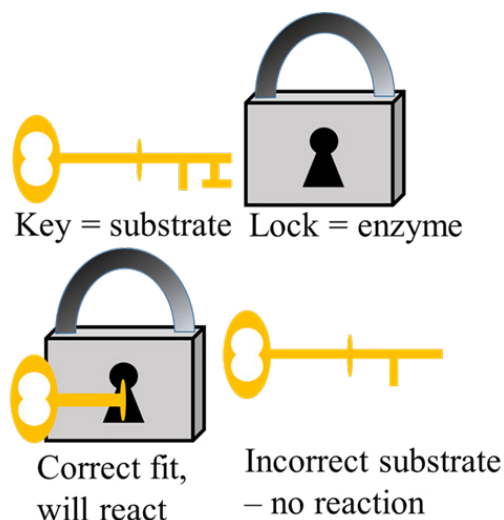


Figure 4. Enzyme “lock+key” model.

substrate will fit into it - like a key into a lock. Once the substrate is fully locked in and in the exact position, the catalysis can begin.

To stop (or slow down) the biochemical activity of the protein, it is crucial to block its active site. For this goal, it is essential to find an appropriate small molecule (inhibitor) that can be docked at the active site of the enzyme and form strong bonds with it (in other words, the energy of interaction between the inhibitor and the protein must be negative with highest possible absolute value). The main challenge is to find this molecule, and so other proteins are not affected.

Computational microscope

In the 300 years since Dutch scientist Antonie van Leeuwenhoek first discovered living cells with his homemade lens in 1674, microscopes have grown hundreds of thousands of times more powerful. Using new methods and techniques, the magnification has moved from the cell to the molecule. In 1997, Klaus Schulten, professor of physics in the University of Illinois at Urbana-Champaign, proposed a new approach that he called “computational microscope”. This method gave birth to modern computational biochemistry. It combines methods of chemistry (molecular structure), physics (potential of interaction between the atoms), and mathematics (algorithms of calculations) with the power of modern supercomputers to provide visualization of the complex biochemical processes at the level of individual atoms. This approach is used in this project. The supercomputing power is achieved through publically available docking internet portals.

Goals and Objectives

The goal of this project is to find or build a small molecule that has a negative energy of interaction with alkaline phosphatase (so that it can attract to and block the active site of the enzyme) and positive energy of interaction (repulsive interaction) with other phosphatases. This inhibitor is a potential drug for bone cancer treatment. Objectives include building models for a set of small molecules (inhibitors) that may be used in chemotherapy, creating a list of phosphatases typical for human cells to compare with alkaline phosphatase, and calculating the energy of interaction between all the inhibitors and proteins.

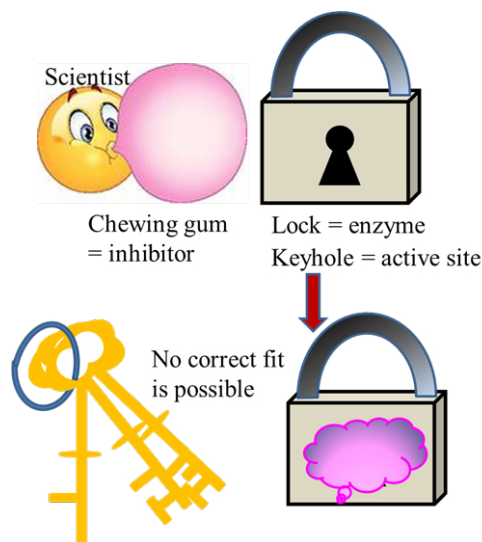


Figure 5. Drug development “lock+key+chewing gum” model.



Figure 6. Portrait of Antonie van Leeuwenhoek (1632–1723) with his microscope (Creative Commons Public Domain).



Figure 7. Klaus Schulten (photo by L. Brian Stauffer, University of Illinois at Urbana-Champaign).

METHODS

Databases

Information about various phosphatases was collected from two open access databases: UniProt (www.uniprot.org) and Protein Data Bank (PDB) (www.rcsb.org). PDB web site was used for the introductory visual analysis of the crystalline structures of various phosphatases to choose the proteins for the analysis. UniProt site was used to collect information about the location of the active sites of the phosphatases and sequences of amino acids near the active sites.

Structural analysis of proteins

To understand the functions of proteins at a molecular level, it is often necessary to determine their three-dimensional structure. This is the topic of the scientific field of structural biology. For structural analysis of proteins, PyMOL and Chimera software have been chosen. PyMOL allows a free educational version and Chimera is a free open access program. I had some problems with saving the result in PyMOL in the proper format, so the structural analysis- recognition of and marking the active site, recognition of sequences of amino acids near the active site, and removing water molecules- was done in Chimera.

Modeling of inhibitors

Molecular models describe atoms as point charges with an associated mass. The interactions between neighboring atoms are described as spring-like interactions (representing chemical bonds). Atoms are assigned coordinates in Cartesian space. The collective mathematical expression is labeled as a possible function and is related to the system internal energy (U), a thermodynamic quantity equal to the sum of potential and kinetic energies. The real structure of a molecule is obtained by minimizing the potential energy. To build three-dimensional inhibitor molecules for analysis of their interaction with phosphatases, Avogadro software was used. This is a free, open source molecular editor and visualization tool software.

List of inhibitors

To compile the lists of inhibitors for analysis of their interaction with proteins, OpenBabel software was used. This free, open source software was developed to

help in the process of interconversion of chemical data from one format to another. Calculation of the energy of interaction between a protein and various inhibitors in AutoDock Vina requires the list of molecules in the format MOL2.

Docking inhibitors

Nowadays, it is well known that most of the processes in life sciences involve, in the atomic scale, complex interactions between at least two molecules. The prediction of such interactions, by so-called docking software, is an important task. The most commonly used software is AutoDock Vina, an open-source program for doing molecular docking. This program does not have a simple user-friendly interface, and several internet portals have been organized over the world to run this program (or other, similar ones) with their own interfaces using supercomputers. In this project, RPBS internet portal located at University of Paris Diderot⁵ was used. It allows calculation of the energy of interaction between the molecules (positive energy corresponds to repulsion and negative energy-attraction) as well as visualization of docking results.

RESULTS

Structural analysis of proteins

Alkaline phosphatase is an enzyme that releases phosphate under alkaline conditions and is made in liver, bone, and other tissues. A test to check the level of alkaline phosphatase is one of the standard tests in cancer diagnostics. The increased level of ALP in cancer cells probably means that this protein is very important for cancer cells. Our main goal is to find small molecules (inhibitors) that can block the biochemical activity of alkaline phosphatase.

However, there are many other phosphatases that are similar to alkaline phosphatase. We want to find molecules that have an attractive interaction (negative energy of interactive) with alkaline phosphatase but a repulsive interaction (positive energy of interaction) with other phosphatases, because we don't want to disrupt the normal function of healthy cells.

For the comparative analysis we chose ten proteins of the phosphatase type that appear in human cells. For all the

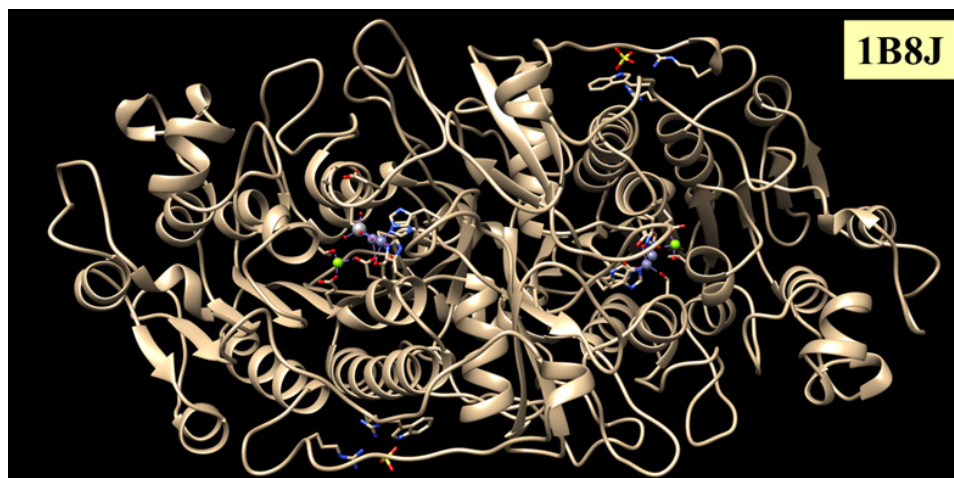


Figure 8. Crystalline structure of alkaline phosphatase.

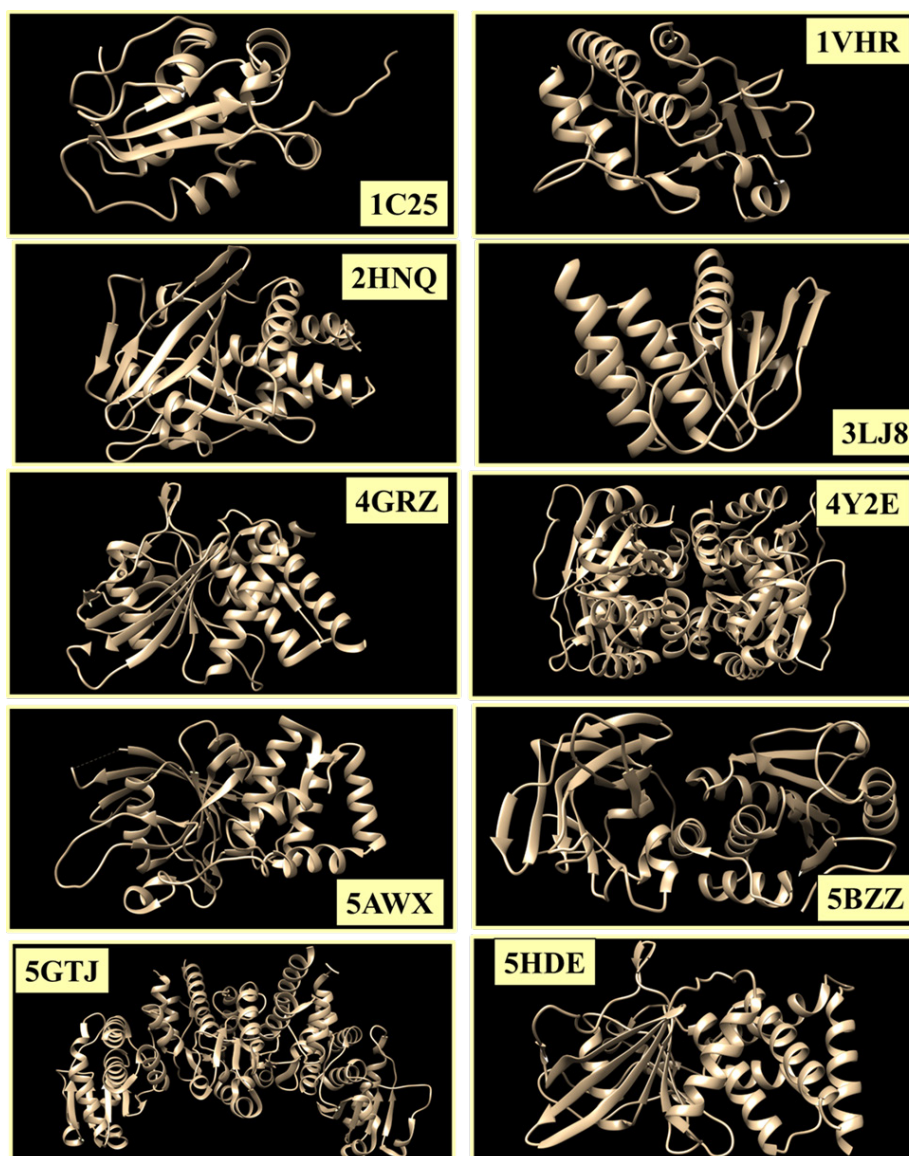


Figure 9. Crystalline structures of the ten considered phosphatases.

Table 1. Location of the active sites of Alkaline phosphatase (1B8J) and ten phosphatases used for comparison.

Protein Code	Active Site	X Coordinate	Y Coordinate	Z Coordinate
1B8J	102	75.006	39.147	41.456
1C25	431	9.694	39.543	68.860
1VHR	124	27.978	44.266	22.475
2HNQ	215	44.380	16.624	9.164
3LJ8	290	14.923	119.274	77.911
4GRZ	453	-17.203	20.798	19.250
4Y2E	232	0.810	-1.082	-1.839
5AWX	1933	25.662	-3.471	0.566
5BZZ	124	-18.698	-37.394	10.901
5HDE	231	11.390	5.495	17.672
5GTJ	152	-11.141	10.827	54.638

Table 2. Sequences of the amino-acids near active sites of the considered proteins. The one-letter abbreviations are given in Table 3.

Protein	Sequence of aminoacids near the active site
1B8J	Y V T D C A A S A T A W S
5AWX:	V V V H C S A G V G R T G
4GRZ:	I I V H C S A G I G R T G
1VHR:	V L V H C R E G Y S R S P
5GTJ:	I L V H C A V G V S R S A
2HNQ:	V V V H C S A G I G R S G
3LJ8	V L V H C L A G V S R S V
4Y2E	V L V H C L A G I S R S V
5BZZ	A A I H C K A G K G R T G
1C25	V V F H C E F S S E R G P
5HDE	I C I H C S A G C G R T G

Table 3. One letter and three-letter abbreviations of the amino-acids.

Amino acid	3-letter abbreviation	1-letter abbreviation
Alanine	Ala	A
Arginine	Arg	R
Asparagine	Asn	N
Aspartic acid	Asp	D
Cysteine	Cys	C
Glutamic acid	Glu	E
Glutamine	Gln	Q
Glycine	Gly	G
Histidine	His	H
Isoleucine	Ile	I
Leucine	Leu	L
Lysine	Lys	K
Methionine	Met	M
Phenylalanine	Phe	F
Proline	Pro	P
Serine	Ser	S
Threonine	Thr	T
Tryptophan	Trp	W
Tyrosine	Tyr	Y
Valine	Val	V

phosphatases we found locations of the active sites, their Cartesian coordinates and compared sequences of amino acids near the active sites. This information is required for the calculation of the energy of interaction between inhibitors and molecules of proteins. The interaction takes place at the active sites of the proteins; active site locations must be reachable for the inhibitors. If the active site is too deep inside the protein core and the size of the active

site pocket is too small, molecules cannot enter.

Inhibitors

To block the active site of alkaline phosphatase, it is crucial to develop small drug-like molecules that selectively inhibit ALP. The choice has been done based on the analysis of experimental data provided in the review of al-Rashida and Iqbal (2015). Twenty five compounds

Table 4. Energy of interaction between inhibitors and phosphatases (in kcal/mol). Bright red, orange, and yellow signify higher positive value and darker colors signify lower absolute value.

Compound	ALP	1C25	1VHR	2HNQ	3LJ8	4Y2E	5AWX	5BZZ	5GTJ	5HDE
KS01	-5.6	-0.2	24.7	2	18.2	3.8	-2.4	2.4	19.9	9
KS02	-4.1	18.4	35	28.8	10.1	29.6	9.6	10.6	18.7	10.6
KS03	-4.1	18.1	34.2	25.5	14.2	29.9	11.9	12.6	24.7	11.7
KS04	-2.1	5.8	30.8	26.3	32.4	17.9	4.7	8.7	25.4	14.2
KS05	1.1	42.3	54.1	55.6	33.2	37.6	28.1	39.7	57.5	23.3
KS06	-2.2	7.2	49.9	43.5	37.2	40.2	16.7	15.4	42.5	18.2
KS07	-5.8	5	38.7	26.2	24	25.7	9.4	11.7	26.6	9.7
KS08	5.1	61.9	91	93.4	81.6	84.1	73.4	65.8	82.6	47.1
KS09	-4.3	14.6	56.8	41.2	27.5	37.1	21.4	30.9	61.7	19.3
KS10	-4.1	14.8	54.6	43.2	35.4	40.1	21.8	29.4	50.5	19.1
KS11	-2.5	47.9	73.6	77.8	50.6	64.8	36.3	45.9	76.2	27.1
KS12	-4.5	14.8	47.8	36.3	41.3	32.6	17.7	20.6	33	14.4
KS13	0.3	21	53.4	53.6	43.3	48.4	25.7	24.6	39.3	20.5
KS14	-3.6	16.3	47.3	42	44.5	37.4	12.7	21.6	42.8	14.3
KS15	-2.1	22.8	58.2	56.9	50.3	46.6	29.6	38.5	62.7	20
KS16	-1.8	15.5	49.5	35.9	44.1	37.3	17	27.8	54.6	14.3
KS17	-2.8	44.1	70.4	73.2	47.8	58.1	38.1	43.1	76.4	26.1
KS18	-1.6	26	58.1	63.7	47.9	46.9	21.4	32.1	41.1	19.4
KS19	-4.2	12.4	45.7	32.3	36.1	34	14.2	20.4	35.6	12.1
KS20	-0.2	29.7	57.4	55.9	46.4	51.5	20.6	32.2	52.2	20.2
KS21	-1	31.7	61.2	61.9	52.8	45.2	24.3	35.7	45.9	21.3
KS22	-1.9	23.9	56.1	59.6	41.8	51.6	26.4	27.4	50.9	20.9
KS23	-2.5	49	74.4	76.7	53.7	59.4	50.3	46.3	77.5	29.1
KS24	-3.8	58.7	75.5	85.4	65.2	67.4	51.8	56.1	79.5	32.8
KS25	6	50.3	64.4	71.5	65.3	71.3	46.7	52.6	66.1	38.7

that form strong bonds with Alkaline Phosphatase were selected and numbered from KS01 to KS25. Then, the 3-D models of these molecules were build using Avogadro software.

Molecular models describe atoms as point charges with an associated mass. The interactions between neighboring atoms are described by spring-like interactions

(representing chemical bonds). Atoms are assigned coordinates in Cartesian space. The collective mathematical expression is termed a potential function and is related to the system internal energy (U), a thermodynamic quantity equal to the sum of potential and kinetic energies.

The shape of the molecules was automatically adjusted

via minimization of the potential function.

Docking the inhibitors

Energy of interaction between proteins and inhibitors was calculated at RPBS web portal that uses AutoDock Vina docking simulation program. Negative energy corresponds to the attractive link between the inhibitor and protein and positive energy means that there is repulsion between them. AutoDock Vina takes into account Coulombic forces between the atoms as well as Van der Waals's forces. RPBS portal also allows visualization of the results. The protein, 4GRZ, did not react with any of the inhibitors since its active site is located too deep inside the protein and the pocket size is too small.

CONCLUSIONS

This project was successful in finding possible inhibitors for ALP that don't block the other phosphatases. The primary goal of this project was to make sure all of the inhibitors had a negative energy of binding to ALP and positive energy of binding to the other phosphatases, because negative numbers mean a high energy of interaction with the active site. We found that most of investigated inhibitors had a negative energy to ALP and can serve as potential drugs for bone cancer.

Methodological conclusion came out of the (successful) docking process. The docking results reproduce the experimentally observed high inhibiting activity of these inhibitors, and such a remarkable agreement between

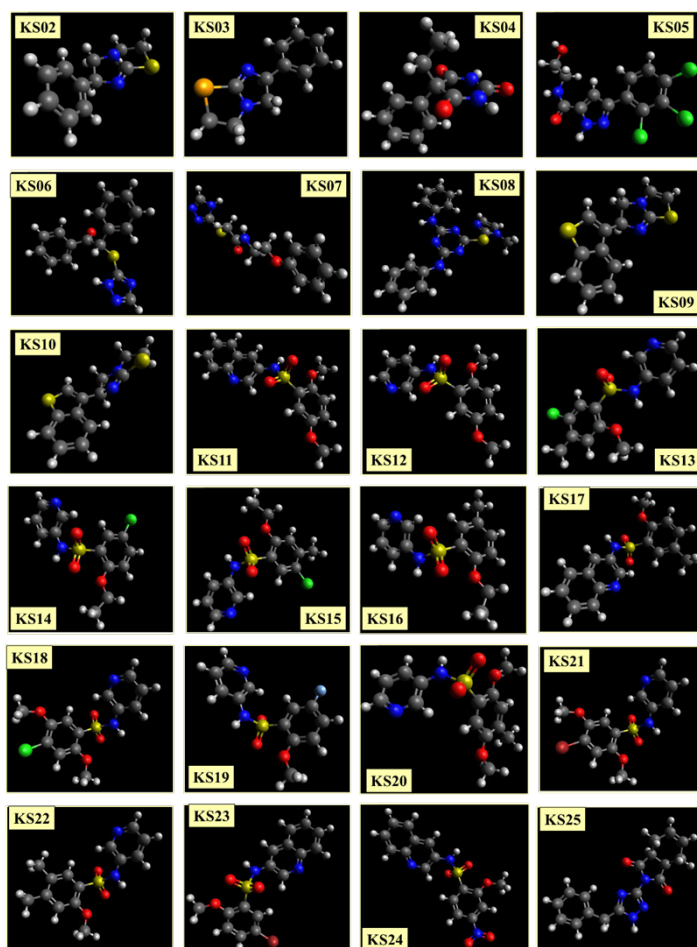


Figure 10. Molecules of the inhibitors used in the project.

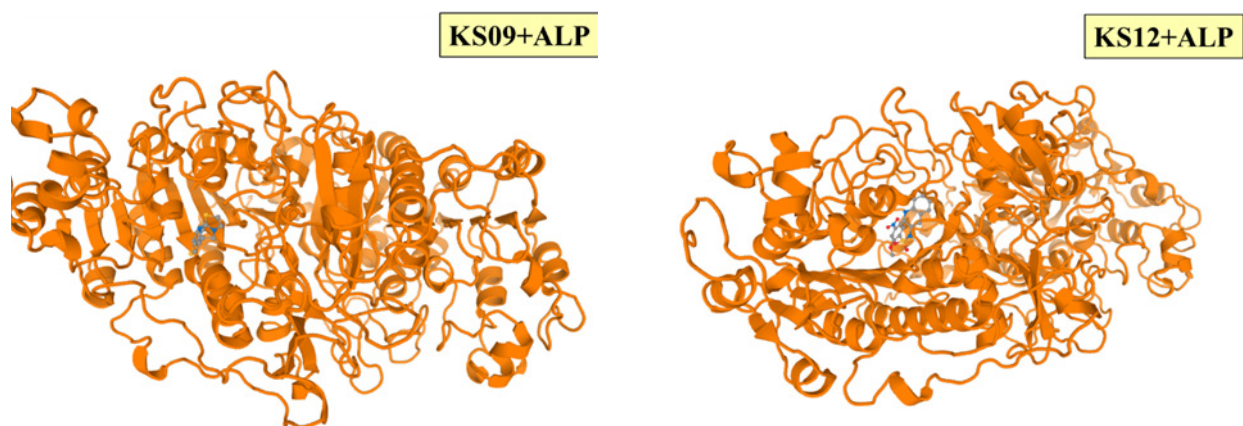


Figure 11. The two best results were obtained for compounds KS09 and KS12. These two inhibitors showed an attractive interaction with alkaline phosphatase and a repulsive interaction with all the other considered proteins.

the experiment and calculations demonstrates the efficiency of our docking process.

We should be able to find differences between the phosphatases to target them with small-molecule inhibitors, which can serve as a possible drug. For this project, we defined a “good” inhibitor by the following terms:

- Negative value of binding to ALP
- Binding energy of at least positive 10 kcal/mol for the other phosphatases

If it had a positive value for ALP it was marked “bad”.

We chose the top five inhibitors by comparing the lowest values for ALP, ranging from -0.2 to -4.5 kcal/mol and took the lowest five.

The hypothesis was correct because we were, in fact, able to find quite a few inhibitors for ALP that did not block the other phosphatases.

ACKNOWLEDGEMENTS

I would like to thank my mentor, Professor Marat Talipov (Department of Chemistry and Biochemistry of NMSU), for his advice and for teaching me to work with chemical software. I would also like to thank my mother and father, friends, and teachers for supporting me through the hard parts of this project and for inspiring me to keep it up.

ENDNOTES

- 1 <https://www.cancer.net/cancer-types/bone-cancer/statistics>
- 2 <https://www.urmc.rochester.edu/encyclopedia>
- 3 Kaplan, 1972, McComb et al, 1979, <https://www.youtube.com/watch?v=Vc2PSR00KfY>
- 4 Miller and Levine, 2010
- 5 <http://mobyle.rpbs.univ-paris-diderot.fr>

REFERENCES

Adult and Children's Health Encyclopedia. University of Rochester Medical Center, 2018, www.urmc.rochester.edu/encyclopedia. Accessed March 2018.

“Alkaline Phosphatase Enzyme.” *YouTube*, uploaded by Aladdin Creations, 6 March 2017, www.youtube.com/watch?v=Vc2PSR00KfY. Accessed March 2018.

Al-Rashida, M. and J. Iqbal. “Inhibition of alkaline phosphatase: an emerging new drug target.” *Mini-Reviews in Medicinal Chemistry*, vol 15, 2015, pp 41-51.

“Bone Cancer: Statistics.” *Cancer.net*. American Society of Clinical Oncology, 2018, www.cancer.net/cancer-types/bone-cancer/statistics. Accessed March 2018.

Davidson, Michael. *Molecular Expressions: Exploring the World of Optics and Microscopy*. Florida State University, 12 September 1995, micro.magnet.fsu.edu. Accessed 2018.

Kaplan, M. M. “Alkaline phosphatase.” *The New England Journal of Medicine*, vol 286, 1972, pp 200-202.

McComb, R.B., Bowers, G.N., Posen, S. *Alkaline Phosphatase*. Plenum Press, 1979.

Miller, K. R. and Levine, J. S. *Biology*. Prentice Hall, 2010.

Néron, B., Ménager, H., Maufrais, C., Joly, N., Maupetit, J., Letort, S., Carrere, S., Tuffery, P., Letondal, C. *Mobyle: A Bioinformatics Framework*. Ressource Parisienne en Bioinformatique Structurale & Institut Pasteur Biology IT Center, 19 November 2009, mobyle.rpbs.univ-paris-diderot.fr. Accessed March 2018.

RCSB Protein Data Bank. Research Collaboratory for Structural Bioinformatics, Rutgers University & the University of California San Diego, 2018, www.rcsb.org. Accessed March 2018.

Theoretical and Computational Biophysics Group. National Institutes for Health Center for Macromolecular Modeling & Bioinformatics, University of Illinois at Urbana-Champaign, 20 March 2006, www.ks.uiuc.edu. Accessed 2018.

UniProt. UniProt Consortium, 2002, www.uniprot.org. Accessed March 2018.

AUTHOR INFORMATION

Ksenia Sevostianov
Sierra Middle School
kseniakitty303@gmail.com

New Mexico Academy of Science 2018 Awards for Outstanding Science Teaching



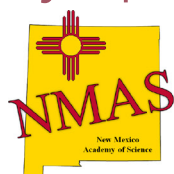
Outstanding Science Teacher winners attend the NMAS 2018 Research Symposium. From left to right: Donovan Porterfield of the Central New Mexico Local Section of the American Chemical Society; 2018 Outstanding Science Teacher recipient Nate Raynor of Mescalero Apache Schools; NMAS President John Emmerson, 2018 Outstanding Science Teacher recipient Julianna Matz-Esquibel of Taos High School.

Outstanding New Mexico Science Teacher Awards honor New Mexico science and math educators, and have been given since 1968. The Academy recognizes teachers who provide opportunities for students to succeed. Nominations are open to all science and math teachers in New Mexico. Prior to 1990, awards were given to a K-12 teacher and a post-secondary instructor. Beginning in 1990, awards were given to two K-12 teachers annually. The American Chemical Society also presents a monetary award and teaching materials to the NMAS winning teachers.

Nate Raynor is a science teacher in the Mescalero Apache Schools, and was nominated by Karen Kinsmen (STEM-H Center for Outreach, Research & Education). Mr. Raynor is one of those teachers that students remember and respect for a lifetime. He truly makes a difference and goes way beyond expectations to engage his students. Nate works tirelessly with students both in and out of the classroom. They have fielded robotics teams, done research projects, and much much more...with terrific success! Nate is committed to making sure his students are well prepared to enter post-secondary education and/or careers when they graduate. This not only includes what happens in the classroom, but also his support for students who may not have a very easy life outside of school.

Julianna Matz-Esquibel is a science teacher at Taos High School, and was nominated by Colin Nicholls (Math & Science Dept. Chair, UNM-Taos). The key attribute which characterizes Julianna is her unwavering commitment to her students. In its broadest aspect this shows as her relentless encouragement and exhortation keeping students going even when they had lost confidence in themselves and wanted to give up. Many students are first generation college goers (or will be when they get there) and don't think they are 'college material'. Julianna debunks this and shows them that they can succeed with college level courses by providing dual-credit, college-level Chemistry classes for her high school students. She works with other high school instructors and the UNM-Taos dual credit program to ensure that when her students graduate high school, they have a head start when they get to college. She has also taught AP Chemistry for at least 15 years, getting students to push themselves to achieve academically in STEM fields and helping them gain access to scholarships and entry into some of the country's finest colleges and STEM programs. Her students know they can count on her and if they have difficulties in their lives she will be supportive and act as a sound role model.

New Mexico Academy of Science Research Symposium



ABOUT THE RESEARCH SYMPOSIUM

The 2018 New Mexico Academy of Science Research Symposium was held in Albuquerque on 27 October 2018. The Symposium was sponsored by the New Mexico Academy of Science (NMAS), the New Mexico Experimental Program to Stimulate Competitive Research (NM EPSCoR), the University of New Mexico Center for Water and the Environment, the American Chemical Society (ACS), and the New Mexico Alliance for Minority Participation (NM AMP). The Symposium schedule included 22 oral presentations and 40 poster offerings from the students and faculty of New Mexico's universities and colleges. The luncheon included the New Mexico Academy of Science's two annual awards for Outstanding Science Teaching, and Dr. Doug Olson of the National Institute of Standards and Technology provided the luncheon keynote address. Abstracts of these presentations are included in this annual volume of the *NMAS New Mexico Journal of Science*. The Symposium closed with the presentation of awards for what were judged to be the best graduate and undergraduate posters. The full agenda is online at www.nmepscor.org/nmas/2018.

KEYNOTE SPEAKER: DOUGLAS OLSON, PHD



Dr. Olson is the Chief of the Office of Weights and Measures at the National Institute of Standards and Technology (NIST). As a career NIST employee, he has served as a bench scientist, technical project leader, and leader of a research group prior to his current position. He is an internationally recognized expert in pressure metrology who has published widely in that area. He represented NIST in a two-year assignment at the International Bureau of Weights and Measures (BIPM) in Paris, where he coordinated mutual recognition aspects of international measurement capabilities. As the Chief of the Office of Weights and Measures, he is responsible for the oversight

of the programs of Laboratory Metrology, Legal Metrology Devices, Laws and Metrics, and International Legal Metrology. Combined, these programs form the United States' coordinated management of legal metrology. As a non-regulatory agency, the NIST Office of Weights and Measures works cooperatively with federal, state, and local regulators, as well as industry, manufacturers, and consumer groups, providing training and technical assistance that covers the broad spectrum of legal metrology.

SYMPOSIUM WELCOME FROM 2018 NMAS PRESIDENT

On behalf of the New Mexico Academy of Science, I would like to welcome each of you to the 2018 Research Symposium! NMAS is pleased to partner with New Mexico EPSCoR, the UNM Center for Water and the Environment, the American Chemical Society, and New Mexico AMP to sponsor this annual conference to promote science and science education in our community. Our keynote speaker is Dr. Doug Olson, Chief of the Office of Weights and Measures at the National Institute of Standards and Technology. He will be speaking about ruminations on his career in measurement standards: metrology, the history of the US weights and measures system, and the new SI. Join us for his lunchtime presentation as well as the awards for Outstanding Teacher in our state, plus a day of interesting and engaging presentations by students and professors, as well as the student poster awards in the afternoon.

John Emerson, NMAS President

ABOUT THE SPONSORS

NEW MEXICO ACADEMY OF SCIENCE

Founded in 1902, the New Mexico Academy of Science has been in continuous existence since 1915. The Academy is a member of the National Association of Academies of Science (NAAS) and an affiliate of the American Association for the Advancement of Science (AAAS). The New Mexico Academy of Science works with teachers, state agencies, and the legislature to establish appropriate standards for the teaching of the sciences. The Academy goals are to foster scientific research and scientific cooperation, increase public awareness of the role of science in human progress and human welfare, and promote science education in New Mexico. Visit www.nmas.org to learn more.

NEW MEXICO EPSCOR

The New Mexico Established Program to Stimulate Competitive Research (NM EPSCoR) is funded by the National Science Foundation (NSF) to build the state's capacity to conduct scientific research. The infrastructure and activities of Energize New Mexico are designed to support shared-use equipment, engage new research and community college faculty, and support the STEM pipeline by training teachers, undergraduate and graduate students, and post-doctoral fellows. Research findings are communicated broadly through various outlets, including local museums. Visit www.nmepscor.org to learn more about NM EPSCoR, and visit www.nsf.gov/epscor to learn more about the NSF EPSCoR initiative and other jurisdictions.

AMERICAN CHEMICAL SOCIETY

The American Chemical Society (ACS) is the world's largest scientific society and one of the world's leading sources of authoritative scientific information. A nonprofit organization, chartered by Congress, ACS is at the forefront of the evolving worldwide chemical enterprise and the premier professional home for chemists, chemical engineers and related professions around the globe. The Central New Mexico Local Section of the American Chemical Society was founded in 1946 and generally serves the northern 2/3rds of the state of New Mexico. The Local Section specifically includes the following New Mexico counties: Bernalillo, Los Alamos, Rio Arriba, San Miguel, Sandoval, Santa Fe, Socorro, Taos, Torrance, and Valencia.

UNM CENTER FOR WATER & THE ENVIRONMENT

The mission of the Center for Water and the Environment at the University of New Mexico (UNM) is to increase the participation of underrepresented minorities (URM) in science, technology, engineering and math (STEM) professions while conducting cutting-edge research into technological and engineering-based solutions to problems with water and the environment, in a framework that considers the social, economic, policy, regulatory, and legal implications. Practical solutions to problems related to water availability in arid environments and in times of drought, and problems associated with energy generation and consumption are particularly relevant, in light of the criticality of these issues to the state of New Mexico, the southwestern United States, and their global importance. Learn more at cwe.unm.edu.

NEW MEXICO ALLIANCE FOR MINORITY PARTICIPATION

Established in 1993 with major funding from the NSF, the New Mexico AMP program is a partnership of the state's two- and four-year colleges and universities, with a primary goal of increasing the number of B.S. degrees awarded to under-represented students in New Mexico. NM AMP supports students with scholarships; research assistantships; professional development; and enhanced teaching, learning, and mentoring experiences. Program activities are designed to attend to individual student retention, development, and progression; support student progression to the STEM workforce and graduate school; and promote the replication of best practices, both within New Mexico and nationally. To learn more, visit www.nmsu.edu/~nmamp/.

CONCURRENT SESSION PRESENTATION ABSTRACTS

SESSION A: ENERGY & EDUCATION

Assessing Curriculum Efficiency Through Monte Carlo Simulation

DAVID TORRES, NORTHERN NEW MEXICO COLLEGE

A Monte Carlo algorithm is designed to predict the average time to graduate by enrolling virtual students in a degree plan. The algorithm can be used to improve graduation rates by identifying bottlenecks in a degree plan (e.g., low pass rate courses and prerequisites). Random numbers are used to determine whether students pass or fail classes by comparing them to institutional pass rates. Courses cannot be taken unless prerequisites and corequisites are satisfied. The output of the algorithm generates a relative frequency distribution which plots the number of students who graduate by semester. Pass rates of courses can be changed to determine the courses that have the greatest impact on the time to graduate. Prerequisites can also be removed to determine whether certain prerequisites significantly affect the time to graduate.

Keywords: curriculum efficiency, Monte Carlo simulation, algorithms

Biomass Burning Aerosols and Air Quality in the Southwest U.S.

KIP CARRICO, NEW MEXICO TECH

U.S. efforts over the past several decades to control air pollution emissions have been largely successful in improving ambient air quality in urban areas. Contrastingly, emerging regional trends demonstrate increasing impacts from biomass burning emissions in the southwest US. Though traditionally considered a 'natural' source, stronger links of smoke to a changing climate and other human perturbations are emerging. Our research in collaboration with Los Alamos National Lab researchers, has completed over 300 combustion experiments with a selection of native and invasive plant species from New Mexico. The presentation will discuss such trends and present specific results on the detailed physical properties of smoke aerosols and their significance. Particle size distribution, light scattering, and light absorbing properties of aerosol particles play a vital role in determining aerosol impacts. Such aerosol physical properties, and their relation to external influences such as humidity and combustion characteristics, determine the resulting aerosol impacts on human health, visibility, atmospheric chemistry and significance to climate. Results to date and future efforts will be discussed.

Keywords: biomass smoke, climate, air quality

The Development of a System to Measure Humidity-Dependence of Aerosol Optical Properties

JARED LAM, NEW MEXICO TECH

Aerosols scatter and absorb radiation entering the Earth's atmosphere, which results in either a cooling or a warming effect, respectively. For many aerosol species, these optical properties are influenced by the ambient relative humidity (RH). As particles swell with increasing RH, light scattering increases and aerosol intensive optical properties are altered. At deliquescence humidity, the particle experiences significant growth and consequent effects on its optical properties. The magnitude of this humidity-dependence is a result of heterogeneity of aerosol chemical composition. We have developed a system to measure the humidity-dependence of aerosol optical properties by alternating between dried (RH<20%) and humidified (RH>80%) conditions to measure hygroscopic growth factor $f(RH)$ for light scattering and absorption. The optical properties are measured by a Cavity-Attenuated Phase Shift spectrometer (CAPS PMex) which is designed to measure light-scattering and -extinction by particles at a wavelength of 450nm. Differencing light extinction and scattering gives light-absorption, a parameter whose RH dependence is highly

uncertain. In concert with other aerosol chemical and physical measurements, this improves the scientific understanding of the influence of aerosols on climate change.

Keywords: climate change, engineering, environment

Perspectives on Publishing: Peer Review, Impact, Significance

LAWRENCE BERLINER, UNIVERSITY OF DENVER

The author is Editor in Chief of two international journals: Cell Biochemistry and Biophysics and The Protein Journal. The talk will discuss: purpose of writing (what is a) scientific paper; Why publish? Key Elements of Publishing; Structure of a paper; Peer review - What is it? Scientific fraud has become a major problem; What journal to choose? Rules for the future for successful science and papers.

Keywords: peer review, publishing, higher education

SESSION B: CHEMISTRY I

Photophysical Properties of Radical Elaborated Donor-Acceptor Pt Complexes

RANJANA DANGI, UNIVERSITY OF NEW MEXICO

Square planar donor-acceptor platinum complexes have garnered considerable interest due to their rich photochemical properties and their photoluminescence behavior. These complexes possess a low energy Donor \rightarrow Acceptor ligand-to-ligand charge transfer transition that effectively creates charge separated singlet biradicals in the electronic excited state. Herein, we describe a new molecular framework to probe the effects of excited state lifetimes as a function of radical elaboration. Importantly, these new complexes will allow for detailed interrogation by magnetic circular dichroism (MCD) spectroscopy to understand their electronic structure and time-resolved spectroscopies to understand their excited state lifetimes and dynamics. Understanding these complex excited state interactions is crucial for the further development of improved solar cells, molecular electronics applications, and spintronics. The excited states of these complexes are emissive and indicate long-lived excited states can be achieved. In this presentation, we will discuss our latest photophysical results, which have been interpreted in the context of quantum chemical computations.

Keywords: donor, acceptor, radical, platinum

Ground State Nuclear Magnetic Resonance Chemical Shifts Predict Charge-Separated Excited State Lifetimes

JING YANG, UNIVERSITY OF NEW MEXICO

Dichalcogenolene platinum(II) diimine complexes, (LE,E')Pt(bpy), are characterized by charge separated dichalcogenolene donor (LE,E') \rightarrow diimine acceptor (bpy) ligand-to-ligand charge transfer (LL'CT) excited states that lead to their interesting photophysics and potential use in solar energy conversion applications. Despite the intense interest in these complexes, the chalcogen dependence on the lifetime of the triplet LL'CT excited state remains unexplained. Three new (LE,E')Pt(bpy) complexes with mixed chalcogen donors exhibit decay rates that are dominated by a spin-orbit mediated nonradiative pathway, the magnitude of which is proportional to the anisotropic covalency provided by the mixed-chalcogen donor ligand environment. This anisotropic covalency is dramatically revealed in the ^{13}C NMR chemical shifts of the donor carbons that bear the chalcogens and is further probed by S K-edge XAS. Remarkably, the NMR chemical shift differences also correlate with the spin-orbit matrix element that connects the triplet excited state with the ground state. Consequently, triplet LL'CT excited state lifetimes are proportional to both functions, demonstrating that specific ground state NMR chemical shifts can be used to evaluate spin-orbit coupling contributions to excited state lifetimes.

Keywords: nuclear magnetic resonance, excited state lifetime, Spin-orbit coupling, Ligand-to-ligand charge transfer

Model Studies Address the Geometric and Electronic Structure of a Key Dimethyl Sulfoxide Reductase (Dmsor) Enzyme Intermediate

KHADANAND KC, UNIVERSITY OF NEW MEXICO

Dimethyl sulfoxide reductase (DMSOr) catalyzes the reduction of DMSO to volatile dimethyl sulfide (DMS), playing a vital role in geochemical sulfur cycles. The product, DMS, is a compound of increasing environmental importance that facilitates cloud formation and albedo. The paramagnetic Mo(V) “high-g split” intermediate has been studied by electronic absorption, magnetic circular dichroism, and electron paramagnetic resonance spectroscopies with the data being interpreted as deriving from a 6-coordinate low-symmetry intermediate along the electron transfer half reaction of the enzyme. However, a recent EXAFS study has suggested that this intermediate is 5-coordinate and is off the catalytic pathway. To resolve these issues, we have synthesized new 6-coordinate model compounds for the DMSOr “high-g split” intermediate. A combination of electronic absorption, EPR, and XAS spectroscopic studies have been performed on these models and interpreted in the context of all available enzyme data. We conclude that a 6-coordinate structure is most likely for this intermediate. An interesting inverted bonding scheme is proposed that addresses the electron transfer reactivity of this site in the reductive half reaction of the enzyme.

Keywords: inorganic chemistry, enzymes, intermediate modeling

Probing the Active Site of a Novel Molybdenum Enzyme

LAURA INGERSOL, UNIVERSITY OF NEW MEXICO

Molybdoenzymes possess a unique molybdopterin cofactor and they catalyze a large number of different reactions that are important for the biogeochemical cycles of the most abundant elements of the Earth, such as N, S, C, Cl, as well as playing critical roles in metabolic cycles. YedY is a novel bacterial molybdoenzyme; a putative methionine sulfoxide reductase capable of rescuing proteins damaged by reactive chlorine species. Although YedY exhibits several commonalities with other molybdoenzymes, it has characteristic differences in its electronic structure that make it distinct. Despite structural similarities to sulfite oxidase (SO), YedY cannot catalyze the same reactions and functions as a sulfoxide reductase in vitro. It is the only molybdoenzyme known that is isolated in the paramagnetic Mo(V) oxidation state. YedY possesses an atypical axial EPR spectrum at X-band frequencies that displays an unusually high g_1 value for a molybdoenzyme. Unlike other molybdoenzymes that oxidize and reduce substrates through mechanisms that cycle Mo through its Mo(IV), Mo(V), and Mo(VI) oxidation states, there is no evidence that YedY can be oxidized to the Mo(VI) oxidation state observed for all other SO family enzymes in their catalytic cycles. It has been proposed that YedY instead employs a unique mechanism by which oxidation state changes occur on the ubiquitous pyranopterin dithiolene (PDT) ligand; the Mo ion remaining in the reduced Mo(IV) oxidation state throughout the catalytic cycle. In this work, we utilize a combination of spectroscopy, site-directed mutagenesis of various active site residues, and computations to address these ambiguities.

Keywords: molybdoenzyme, EPR, spectroscopy, mutagenesis

SESSION C: ENGINEERING & MATERIALS SCIENCE

Spark Plasma Sintering of Oxide Dispersion Strengthened Alloys

GEMMA STRONG, UNIVERSITY OF NEW MEXICO

Oxide dispersion strengthened (ODS) alloys are among the most promising candidates for advanced reactor concepts that require higher operating temperatures and irradiation doses. ODS alloys show very high strength, high temperature creep resistance, and highly resistant to irradiation induced damage such as swelling and hardening when uniform dispersion of very fine (1-2 nm) oxide particles and ultrafine grain size obtained such as in 14YWT. However, nuclear reactor applications require complex geometries that require welding. Conventional fusion welding techniques result in significantly altered microstructure (coarsening of particles, change in grain size) due to melting.

Moreover, most ODS alloys have a highly alloyed matrix which makes it difficult to fusion weld. On the other hand, solid state welding techniques such as friction welding, diffusion welding, brazing, etc. were tested with some success. Spark plasma sintering, previously successfully used by us for the consolidation of ODS alloys, is also one of the promising techniques for joining of ODS alloys. The SPS-Joining technique involves application of rapid heating, external pressure, and possible passing of pulsed electric current through the material interface subjected to joining. In this study, SPS was successfully applied to join ODS alloy at different temperature and pressure. We used nanoin-dentation and electron microscopy to characterize SPS joints. Initial investigations indicate uniform properties across the joints. Successful implementation of the SPS joining testing of the joints will remove a major obstacle and allow wide range use of ODS alloys in nuclear applications.

Keywords: nuclear materials science, alloys, oxide

Control of Crystallization and Microphase Separation of Fully Conjugated Block Copolymers by Random Copolymers

YOUNGMIN LEE, NEW MEXICO TECH

Donor–acceptor fully conjugated block copolymers consisting of electron donor and acceptor conjugated polymers are interesting as single-component active-layer materials for solar cells because it can adopt mesoscale microphase separated structures with length scales comparable to the exciton diffusion length. Nevertheless, due to the strong crystallization of poly(3-hexylthiophene-2,5-diyl) (P3HT), morphologies of fully conjugated block copolymers containing P3HT are predominantly driven by crystallization as opposed to microphase separation. We control the crystallization to promote microphase separated structures in fully conjugated block copolymers through the addition of small amounts of 3-octylthiophene to the polymerization of P3HT. Poly(3-hexylthiophene-2,5-diyl-r-3-octylthiophene-2,5-diyl)-block-poly((9,9-dioctylfluorene-2,7-diyl)-alt-(4,7-di(thiophene-2-yl)-2,1,3-benzothiazole)-5,5”-diyl) (P3HT-b-PFTBT) copolymers were prepared by Grignard metathesis followed by chain extension through a Suzuki-Miyaura polycondensation. We demonstrate that a fully conjugated block copolymer incorporating a random copolymer can control crystallization and microphase separation, in result, lead to enhanced performance in solar cell devices.

Keywords: chemical engineering, polymer, solar cells

Lead Selenide Quantum Dots for Use in Solid-State Radiation Detectors

TOM NAKOTTE, NEW MEXICO STATE UNIVERSITY

The unique optical and electrical properties of lead selenide (PbSe) quantum dots (QDs); which are due to quantum confinement effects that are a product of their nanometer scale sizes, have made PbSe QDs an interesting material for various devices from solar cells to photodetectors. Here we aim to leverage another important property, the high Z number of the material, to fabricate solid-state radiation detectors for high energy waves such as x-rays and gamma-rays. PbSe QDs are prepared using colloidal synthesis techniques which employ a weakly binding oleylamine ligand as the stabilizing ligand, for the purpose of fabricating a solid-state radiation detector using PbSe QDs as both the blocking and detection layers. Using oleylamine rather than the more traditional strongly binding oleate ligand allows for the facile in-solution ligand exchange with shorter anionic ligands. QDs passivated with shorter ligands are then implemented into testing devices (such as FETs, capacitors, and simple photodetectors) by spin-coating the colloidal solution into films. Thicker films, which are necessary for attenuation of x-rays and gamma-rays, can be fabricated by using more concentrated solutions and slower spin speeds; without the need for additional layer-by-layer ligand exchange steps, which has hampered and prolonged the fabrication time of thick QD films in the past. Data collected from research devices, such as carrier mobility and carrier capacity, is then used to calculate the performance and assess the feasibility of PbSe QDs as a material for use in low-cost solution processed solid-state radiation detectors.

Keywords: colloidal synthesis, PbSe, quantum dots, radiation detection

Playing Hide and Seek: Physical Factors Influencing the Presence of Submerged Macrophytes in the Jemez Mountains

VIRGINA THOMPSON, UNIVERSITY OF NEW MEXICO

Although not a ubiquitous aquatic ecosystem component, when present submerged aquatic macrophytes (SAMs) perform the key functions of water quality enhancement, habitat structure, food resources, and nutrient cycling. Normally catalogued and studied in lower elevation areas, little is known about SAMs in high elevation areas. We observed SAMs in multiple higher elevation (>2,500 m) stream systems in the Jemez Mountains. We investigated whether elevation alone or a combination of elevation and other factors determines the presence of SAMs at high elevation. We measured physical characteristics (depth, width, velocity, estimated discharge, canopy cover, elevation and stream gradient) of 15 different study locations on three river systems (East Fork Jemez, San Antonio, and Guadalupe/Cebolla) that were chosen based on an assessment using digital orthography. Univariate and multivariate statistical analyses (Mann-Whitney U, PCA, discriminant function analysis) were conducted to determine which combinations of the measured physical factors are most likely to promote SAMs in the Jemez Mountain river systems. SAMs were not present at all sites, and our analyses were able to predict with greater than 87% accuracy the combinations of factors that allow the two most dominant SAM species to exist in the field. We found that deeper, slower moving, narrower, lower gradient stream reaches in the Jemez were the most likely to host SAMs. These factors are similar to those found to control SAM presence at lower elevations, illustrating that growing at high elevation alone did not change the control of these factors on the presence of SAMs.

Keywords: submerged aquatic macrophytes; aquatic ecosystems; high elevation; presence/absence; modeling

Dynamic Pilot-Scale Algal Turf Scrubber® on Dairy Wastewater by Microbial Community Analysis

JUCHAO YAN, EASTERN NEW MEXICO UNIVERSITY

Algal turf scrubber® (ATS) is a cost-effective and point- and non-point source treatment method for recycling the aquatic nutrients while producing biomass suitable for various applications. However, its global deployment is not implemented. Uncontrolled microbial communities, typical of outdoor operations that result in low biomass productivity and poor biomass quality, seems to be the primary reason. To address this, researchers need to explore the optimal algal/bacterial assemblages, conducive to the highest biomass productivity and most efficient nutrient removal and adaptable to local conditions (including climate and wastewater characteristics). In this talk, we present our recent taxonomic and metagenomic analyses for the algal/bacterial communities at four sampling locations of our ATS on dairy wastewater. The sampling intervals were 20 ft down a 100 ft floway. For taxonomic analyses, duplicate samples were collected in October 2017. *Stigeoclonium* sp. and *Cladophora* sp. were two dominant filamentous species. *Stigeoclonium* sp. became more dominant than *Cladophora* sp. at 60 and 80 ft. *Gomphonema* sp. was the dominant diatom at all four sampling locations, but became less abundant along the floway. *Oscillatoria* sp. began to appear at 60 and 80 ft, but in very low abundance. For metagenomic analyses, replicate samples were collected in the end of July 2017. *Phormidium* and *pseudanabaenaceae* were organisms highly represented at 20 ft. *Bacteroidales*, *bacteroidaceae*, and *burkoldaria* were organisms highly represented at 60 and 80 ft. Interestingly, our results show that ATS is a highly dynamic system, whereby sulfur-based metabolism appears to dominate the initial floway then converts to a nitrogen-based metabolism at the terminal end.

Keywords: Algal turf scrubber®, dairy wastewater, and microbial community

Prevalence of *Wolbachia* in field-caught *Aedes aegypti* mosquitoes

ADITI KULKARNI, NEW MEXICO STATE UNIVERSITY

Wolbachia species are natural endosymbionts of approximately 60% of all insect species. The bacteria can manipulate host reproduction through a mechanism known as cytoplasmic incompatibility. Furthermore, certain *Wolbachia* strains can interfere with viral replications in infected mosquitoes. The mosquito *Aedes albopictus* is commonly infected with *Wolbachia*. However, it is controversial if a natural *Wolbachia* infection exists in *Aedes aegypti*, a primary vector for arboviruses including dengue and Zika virus. During a microbial survey in field caught *Ae. aegypti* from New Mexico, *Wolbachia* infection was identified by *Wolbachia* diagnostic PCR assays. *Wolbachia* infected *Ae. aegypti* were detected in samples collected in all eight surveyed locations during May-October 2017. *Wolbachia* prevalence at these locations ranged from 15-100%, with an average prevalence of 57.4% among the 148 individuals screened. Further, we have also identified *Wolbachia* from the wild-caught *Ae. aegypti* from St. Augustine, Florida, with a low prevalence of 4.3%. These bacteria were however not detected in *Ae. aegypti* populations from Deer Park, Harris County, Texas. A *Wolbachia* infected *Ae. aegypti* colony has been initiated, which provides an opportunity to study the impact of the natural *Wolbachia* infection on various life traits of this mosquito vector.

Keywords: *Aedes aegypti*, *Wolbachia*, mosquito vector

Probability of Sex Change in Fishes

BRIAN PASKO, EASTERN NEW MEXICO UNIVERSITY

Fish stocks are in decline worldwide. Despite a large science for the study of population dynamics, management practices appear insufficient to sustain populations. Many important fish species change sex as part of their life cycle. This change affects the dynamics of a population and therefore can effect both the sustainability of a fishery as well as the health and continuance of a species in general. Various social and environmental cues contribute to sex change in such species, including encounter rate between individuals. How an individual female processes these cues affects when/if that female changes sex. We will present the results from a computer simulation that models a territorial, harem, protogynous species. This simulation explores the probability that a female will change sex under several different stimulus processing models. This simulation includes a male, an alpha female (the sex-changing agent) and a number of subordinate females moving in hexagonal territories. These agents move according to rules that simultaneously maximize number of interactions while minimizing time between interactions. We find that the probability of sex change is very sensitive to both territory size and the encounter rate threshold model at action.

Keywords: behavioral ecology, computer simulation, sex-changing fishes

SESSION E: CHEMISTRY II

Hierarchical Zinc Oxide Nanostructures for the Photochemical Reduction of Bicarbonate to Solar Fuels

HANQING PAN, NEW MEXICO TECH

Zinc oxide (ZnO) is an earth abundant, non-toxic, and low-cost material that has been used widely for photocatalytic water splitting, gas sensing, and dye degradation. In this study, several ZnO structures were synthesized, characterized, and tested for the photocatalytic reduction of bicarbonate to formic acid, an intermediate to methanol, a high-octane number fuel. The different ZnO morphologies studied included micron- and nano-particulate ZnO, rods, wires, belts, and flowers. ZnO was also synthesized from the direct calcination of zinc acetate, which provided a cheap and large-scale synthesis method to produce ZnO. The photocatalytic efficiency of the synthesized ZnO was compared to commercial micron- and nano-particulate ZnO, and was proven to be just as efficient. ZnO flowers, possessing the largest surface area of 12.9 m²/g, were found to be the most efficient reaching an apparent quantum efficiency (AQE) of 10.04±0.09%, with a superior performance over commercial TiO₂ (P25), a benchmark photocatalyst. Green

chemistry solvent, glycerol, proved to be a far superior hole scavenger in comparison to 2-propanol, which is derived from petroleum sources. This is the first study to compare different shapes and sizes of ZnO for bicarbonate reduction in an aqueous system with excellent photocatalytic performance.

Keywords: bicarbonate photoreduction, solar fuels, ZnO nanostructures, zincite

A Charge-Separated Diamondoid Metal-Organic Framework for Selective Gas Separation

SHEELA THAPA, UNIVERSITY OF NEW MEXICO

Metal-Organic Frameworks (MOFs) are porous coordination polymers formed by linking metal ions to a variety of ligands. These materials have applications in many fields, including gas storage, gas separation, catalysis, and sensors, due to their unique properties, such as porosity, high surface area, low density, stability and rigidity. Most reported MOFs contain neutral clusters with limited local electric fields, resulting in weak interactions with the incoming guest molecules. However, some MOFs are ionic with isolated charges, either positive or negative, containing pore clogging counter ions that result in limited pore availability. Charge separated, or zwitterionic, MOFs are ionic MOFs containing positive and negative charges, separated at fixed distances, that possess favorable electrostatic interactions with the guest molecules. Herein, we report the synthesis, characterization and gas adsorption analysis of a zwitterionic diamondoid MOF prepared by coordinating an anionic borate ligand to a cationic Cu(I) metal. The resulting MOF was four-fold interpenetrated with a significantly larger BET surface area of 621 m²/g and high environmental stability due to the absence of free ions. At 313 K and under 1 bar pressure, the CO₂ adsorption isotherm of this MOF displayed a temperature dependent adsorption/desorption hysteresis and CO₂/N₂ ideal selectivity of up to 99. The isosteric heat of CO₂ adsorption at zero coverage was 15.85 KJ/mol, confirming the pure physical interaction of MOF during adsorption. The high CO₂ uptake at 313 K, excellent environmental stability, and reasonable heat of adsorption makes this MOF a potential adsorbent for flue gas treatment in the future.

Keywords: Metal-Organic Framework, BET surface area, selectivity

Controlled Nanomorphology of Hybrid Organic/Inorganic Multi-Component Composites through Cooperative Non-Covalent Interactions

LINGYAO MENG, UNIVERSITY OF NEW MEXICO

Hybrid organic–inorganic nanocomposite polymers, with inorganic nanoparticles embedded in organic matrix have emerged as a special category of multifunctional materials. With rational materials design, these hybrids can show the synergistic effect of the properties from both phases. Homogeneous dispersion and orderly arrangement of the organic and inorganic components are key in their functionalities. By controlling the interface and corresponding interfacial interactions between the organic and inorganic entities, we have developed a logical approach to form stable and controlled hybrid nanofiber structures. We demonstrate the formation of hybrid polymer/quantum dots (or iron oxide nanoparticles) nanocomposites through non-covalent interactions (hydrogen bonding, ionic interactions, etc.). We show that by synthesizing conjugated polymers with specific functionalities, capping nanoparticles with different ligands, we can specifically assemble them into a well-ordered core/shell structure. Besides possessing the excellent conducting properties of the polymer, the resulting nanocomposites also show some added value, such as broader light absorption range when combined with PbS quantum dots, magnetic properties when combined with iron oxide nanoparticles. Further characterization under solar cell operation condition demonstrates their potential application for solar energy harvesting. We believe that this composite nanofiber strategy could be used to generate a wide variety of polymer/nanoparticle hybrid nanocomposites. Also, the achievement of homogeneous dispersion of inorganic species into a polymer matrix may offer opportunities to build a unified hybrid nanocomposite platform for different technical applications.

Keywords: organic photovoltaic, conjugated polymer, quantum dot, magnetic nanoparticles, self-assembly

Bluetooth Operation Verification via Monitoring the Transmission Pattern Using Machine Learning

ABDELRAHMAN ELKANISHY, NEW MEXICO STATE UNIVERSITY

Bluetooth is a widely-used wireless communication protocol in small portable devices due to its low energy consumption and high transfer rates. Manufacturers normally buy their Bluetooth chips from third-party suppliers, which are then integrated into a complex hardware-software stack with a variety of potential vulnerabilities. Direct measurement of the output can help security functions prevent unauthorized data transmission. This work proposes a compact supervisory circuit to classify the operation of a Bluetooth chip at low frequencies by monitoring the radio frequency (RF) output of the Bluetooth chip through an envelope detector. The idea is that the envelope detector and classification algorithm can be inexpensively fabricated on a low-frequency integrated circuit in legacy technology and/or with minimal area. When the supervisory circuit detects abnormal behavior, it can be configured to shut down the Bluetooth chip. Using features extracted from the envelope of the RF output signal, we are able to train several machine learning (ML) algorithms to classify different Bluetooth operation modes and parameters such as operation profile, distance between the paired devices, and number of connected devices. In this work, we demonstrate ML models that can separate Bluetooth advertising and transmit/receive modes with ~100% accuracy and classify the operation profile of the Bluetooth chip with ~100% accuracy.

Keywords: Bluetooth, machine learning, security, RF signals, and supervisory circuit

Detection and Verification of Periodontal Pathogens through Real Time PCR

NIKITA DOUGAN, UNIVERSITY OF NEW MEXICO

The detection and verification of *Streptococcus gordonii*, *Fusobacterium nucleatum*, and other oral bacteria is crucial to scientific research involving periodontal diseases and can be done using a Quantitative Polymerase Chain Reaction (Q-PCR) experiment. Experimentation using Q-PCR provides fast and accurate bacterial strain detection over a span of two to six hours [1] compared to traditional microbiology techniques which may take up to 48 hours or more. This research project focuses on the detection and quantification of *S. gordonii*, *F. nucleatum*, and compound biofilms of both bacteria before and after the application of an experimental antimicrobial agent. The quantification of these bacteria through Q-PCR is important in detecting contamination of the experimental samples and in verifying the specific species of bacteria present in a sample. In order to confirm that the bacteria cultures have not been contaminated, a Q-PCR thermal cycler will be used for accurate testing conditions and analyses. Two gene-specific primers for both bacteria are required to amplify the bacteria to a detectable level. Results of the Q-PCR experiments will be determined through the analysis of the graph produced by the StepOnePlus Q-PCR machine and electrophoresis of the samples. Samples that are successfully amplified and confirmed to be either *S. gordonii* and/or *F. nucleatum* are expected to fluoresce and be detected during the reaction. Samples of bacteria, following verification through Q-PCR and electrophoresis, will be used for testing in further research in developing antimicrobial oral products.

Keywords: Q-PCR, PCR, primer, DNA template, S. gordonii, F. Nucleatum, quencher, reporter dye

Mineralogy Controlled Dissolution of Uranium from Airborne Dust in Simulated Lung Fluids (SLFs) and Possible Health Implications

ESHANI HETTIARACHCHI, NEW MEXICO TECH

The recent increase in cardiovascular and metabolic disease in the Navajo population residing close to the Grants Mining District (GMD) in New Mexico is suggested to be due to exposure to environmental contaminants, in particular uranium in respirable dusts (fine dust small enough to reach gas exchanging/ alveolar region of lungs). However, the chemistry of uranium-containing-dust dissolution in lung fluids and the role of mineralogy are poorly

understood, as is their impact on toxic effects. The current study is focused on the dissolution of respirable-sized U-containing-dust, collected from several sites near Jackpile and St. Anthony mines in the GMD, in two simulated lung fluids (SLFs): Gambel's solution (GS) and Artificial Lysosomal Fluid (ALF). We observe that the respirable dust includes uranium minerals that yield the uranyl cation, UO_2^{2+} , as the primary dissolved species in these fluids. Dust rich with minerals uraninite and carnotite is more soluble in GS, which mimics interstitial conditions of the lungs. In contrast, dust with low uraninite and high kaolinite is more soluble in ALF, which simulates the alveolar macrophage environment during phagocytosis. Moreover, geochemical modeling, performed using PHREEQC, is in good agreement with our experimental results. Thus, the current study highlights the importance of site-specific toxicological assessments across mining districts with the focus on their mineralogical differences.

Keywords: uranium, lung fluids, heavy metal inhalation

UNDERGRADUATE STUDENT POSTER ABSTRACTS

Poster session participants are listed alphabetically by last name of registered presenter. * indicates the poster received an outstanding Undergraduate poster award at the NMAAS 2018 Research Symposium.

Spikerbox DIY

LEVI ALBERT, NORTHERN NEW MEXICO COLLEGE

STEVE COX, NORTHERN NEW MEXICO COLLEGE

JASON LEWIS, NORTHERN NEW MEXICO COLLEGE

ULISES RICOY, NORTHERN NEW MEXICO COLLEGE

We are duplicating Backyard Brain's Spikerbox to further understand how it works, and how it can be used to educate the public about neuroscience. The Spikerbox takes neuron signals from a cockroach leg converts them into an audio signal and transmits them to a speaker, so the viewer can hear the neurons ticking as the leg is touched. This is to help understand the neurological connections within insects. We are taking a pre-made instruction guide and building our circuit from spare parts laying around our engineering building. With help from our faculty and fellow Northern students, we can design and build our circuit, as well as being able to test it with a Spikerbox alongside to compare the output signals. Most of our components needed were on hand in our engineering build, others we had to order online. Being that we are both electromechanical engineering students, we were able to construct the circuit with relative ease. As we are halfway through our project, it is not yet complete. We are expecting a fully operational Spikerbox duplicate by the end of the year. We will be able to take a leg of a cockroach and transmit the neuron signals from its leg to a speaker of ours. The design will be different, as we are building from scratch, so we will most likely design a box for it to be placed in.

Keywords: Spikerbox, cockroaches, engineering

Subsurface hydrology of the Earth's largest sand dunes*

SAMANTHA ASCOLI, UNIVERSITY OF NEW MEXICO

XIAOPING YANG, ZHEJIANG UNIVERSITY

LOUIS SCUDERI, UNIVERSITY OF NEW MEXICO

Understanding the subsurface hydrology, or ground water elevation, of arid environments like large dune forming deserts, is critical to sustaining habitable zones during times of rapid climate change. The tallest dunes and largest sand sea in the solar system is located on Earth, in China's Badain Jaran Desert. The Badain Jaran Desert provides a unique study area because it has been inhabited by human populations since prehistoric times, and provides a unique opportunity to utilize both geologic and archaeological evidence for indicators of Quaternary climate change over the past 5,000 years. We hypothesize that the decrease in water table elevation reflected in modern interdune lakes is a result of Quaternary climate change, transforming the region from wetlands to an arid dune complex. Although this area has a rich archaeological record, limited studies have been conducted to understand the modern water table elevation and its change through recent Earth history. Using satellite imagery and geospatial processing and analyzing tools such as ArcGIS and Google Earth, the modern ground water elevation was traced within the dune field and compared to ancient lake core sediment samples. The samples were radio-carbon dated to compare the rate of change in ground water elevation over the past 5,000 years. Utilizing the archaeological record within the study area, we compared the change in human populations within the region to the change in water resources over time and found a relationship between population decrease and a decrease in ground water elevation within the Quaternary.

Keywords: climate change, geology, archaeology, subsurface hydrology, dune complex

Isolation, separation, and identification of antimicrobial compounds from *Ericameria nauseosa*

DANAYARA CHILDRESS, UNM-VALENCIA

VICTOR FRENCH, UNM-VALENCIA

SHANIA SANCHEZ, UNM-VALENCIA

TRACY J. TERRY, UNM-VALENCIA

Antibiotic resistance is one of the biggest public health challenges of our time. Plant extracts are potential new resources for identifying agents that could act as alternatives to traditional antibiotics in the treatment of antibiotic resistant bacteria. We have conducted a survey of the antimicrobial properties of twenty common plants of the

southwest. Of the twenty plants analyzed, five yielded oils via steam distillation. Two of the five oils exhibit antimicrobial activity via Kirby-Bauer assay: *Vitex agnus-castus* and *Ericameria nauseosa*. The distillate of *E. nauseosa*, commonly called chamisa or rabbitbrush, was found to be the most active antimicrobial agent tested with activity against twelve of the thirteen bacteria tested. GC, TLC, and HPLC-MS have been used to separate and identify the components of the oil from *E. nauseosa*. A luminescent bioassay coupled to TLC is being explored for the identification of the active component.

Keywords: antibiotic resistance, southwestern plant extracts, Ericameria nauseosa

Dark septate fungal endophytes

AMANDA DAVIS, WESTERN NEW MEXICO UNIVERSITY

Dark septate endophytes are a type of mycorrhizal fungi that colonize the roots of a variety of different plant species in a symbiotic relationship, *Bouteloua Gracilis* is a species of grass found growing throughout the U.S. It exhibits a close relationship with DSE and is found in abiotically stressful environments. DSE have been documented in ameliorating abiotic stresses to Blue Gramma, specifically concerning soil quality. Just as plant development is dependent upon soil Ph, DSE also have their own responses to soil acidity.

Keywords: endophytes, grass, symbiotic relationships

Expression & purification of SUMO activating enzyme 1 & 2 (SAE 1/SAE 2) for viral protein interaction studies*

JESSE DIRMEYER, WESTERN NEW MEXICO UNIVERSITY

SUMOylation is a post-transcriptional modification system that is essential to numerous cellular functions including DNA repair, cellular response to stress, and transcriptional regulation through the cell cycle. In recent studies, disruptions in the SUMOylation pathway have been shown to have a role in health ailments such as cancer and neurodegenerative disease. SUMO activating enzyme 1 and SUMO activating enzyme 2 (SAE1/SAE2) facilitates the binding of small ubiquitin-like modifier (SUMO) proteins to target proteins, which lead to the modification of their functions. SAE1/SAE2 activity is obstructed by the avian adenoviral protein, GAM1, resulting in the global inhibition of cellular SUMOylation. This study aims to determine the complex structure of the GAM1 and SAE1/SAE2, which would provide useful insight of their interaction and GAM1's role of SUMOylation regulation. For this study, SAE1 and SAE2 were cloned as a single peptide with flexible linker between them in previous studies. The conjugated construct was obtained and transformed into *E. coli* BL21 competent cells. Protein expression protocols were optimized to increase yield and solubility of both the recombinant proteins. Soluble protein was purified using affinity chromatography. A high yield of soluble pure complex will be used for functional and structural studies with purified GAM1 protein that will enhance our understanding of the mechanism behind virus-host protein-protein interaction and possibly revealing a target for anti-viral therapies.

Keywords: viral proteins, DNA, SUMOylation

Ultrasonics for high-accuracy low-cost flow sensing applications

HANSEN DUBÉ, NEW MEXICO TECH

Flow measurement of corrosive liquids such as hot brine is difficult without expensive instrumentation. A low-cost ultrasonic flow sensor was designed and constructed from common plumbing hardware and commercially available ultrasonic transducers and electronics. A bench-scale study was performed to determine the applicability and limitations of the small-scale flow sensing device. Preliminary investigation suggests milliliter per minute resolution at a cost far below commercial solutions. Further study will include verification of flow rate range and resolution.

Keywords: ultrasonics, plumbing, engineering

Node localization using transitional region based distance estimation

TRAVIS FISHER, EASTERN NEW MEXICO UNIVERSITY

With each passing year, all the appliances and devices around us are becoming “smarter”. The Internet of Things (IoT) is created when these devices communicate with each other. One of the key attributes of these smart devices is the ability to know their accurate location. While GPS and other hardware are currently being used for this purpose, cost and energy consumption are major limiting factors on their widespread adoption in the IoT space. Many different distance measurement techniques have been researched for localization, but there is still no perfect solution. In this research, a localization algorithm was proposed. The algorithm is based on transitional region based distance estimation. In a sender's transitional region, the chance for a receiver to receive packets from a sender is reverse proportionate to the distance to the sender; the relationship between packet loss and distance is close to linear. For a network, all nodes estimate their distance to all their neighboring nodes. If some of the nodes know their accurate location as anchoring nodes, the accurate location information for every node can be estimated. The proposed algorithm is tested for 1-dimensional and 2-dimensional IoT deployments.

Keywords: distance estimation, algorithms, GPS alternatives

Research garden experiments reveal the effects of lineages in Pinyon Pine growth and performance

DALYNA HANNAH, NAVAJO TECH

In 2016, in collaboration with Northern Arizona University, a research garden was developed in Navajo Technical University in Crownpoint, New Mexico to study the effects of climate change in the Southwest United States using a foundation species endemic to this region, Pinyon Pine, (*Pinus edulis*). Pinyons used for this study primarily came from two source origins: New Mexico portion of the Navajo Nation (NN) in Borrego Pass, Mariano Lake, Mariano Lake Pass (MLP), and Tsaille and Sunset Crater (SC) in Northern Arizona. Out of 402 seedlings originally planted in the garden, 163 survived and were measured for height, trunk diameter, total shoot growth, and distribution of shoot type (between bract and fascicle shoots) to determine the effects of lineages on pinyon growth and performance. We found that overall NN seedlings outperformed their SC cohorts except on seedling height and bract shoot percentage and MLP seedlings from NN performed better than its NN cohorts. However, similar growth patterns were found between SC seedlings and Borrego Pass seedlings suggesting limited adaptive responses which indicate their possible suitability for use in restoration efforts across diverse habitats over other sources and lineages with less adaptive potential. Integrating belowground measurements with aboveground measurements is recommended in future studies to distinguish which type of response (adaptation, phenotypic plasticity) was/were elicited.

Keywords: Pinyon Pine, plant lineages, ecology

Effects of geomorphology on light penetration in the Rio Grande

MOLLIE HANTTULA, UNIVERSITY OF NEW MEXICO

REBECCA BIXBY, UNIVERSITY OF NEW MEXICO

Light penetration in aridland rivers, such as the Rio Grande, is restricted by parameters including turbidity, depth, and flow. Understanding the relationship among these parameters and light penetration will help provide a better understanding of habitat limitations for primary producers, such as algae; who are dependent on light to support photosynthesis. The purpose of my study is to examine the geomorphology of an aridland river and show the relationships among depth, turbidity, and light penetration to better understand the abiotic factors shaping the producer communities. Two sites were chosen along the Rio Grande in the Albuquerque reach along a gradient of turbidity. Velocity (m/s), depth (cm), light intensity (μmol), and turbidity (NTU) were collected along vertical transects through the water column that were 25 cm or greater in depth. Preliminary results show that changes in turbidity and water depth were significant statistically ($p < 0.05$) when predicting light penetration intensity with light availability

decreasing exponentially at greater depths along the vertical column transect. By understanding the controls of light penetration in turbid waters, future studies can better delineate the limited environments for primary producers often constrained by the geomorphology of aridland rivers.

Keywords: turbidity, light intensity, aridland rivers, geomorphology, abiotic factors, algae

Relationships among wind speed, precipitation and temperature in New Mexico

KENNETH HOKE, MESALANDS COMMUNITY COLLEGE

This study examined data from NOAA NCDC to find seasonal means for wind speed, precipitation and temperatures, and find correlations among the three variables. Automated Surface Observation Systems (ASOS) accumulated the data at 10-meter observation points from three different airports in the State of New Mexico (Clovis, Grants, and Carlsbad). I used long-term data sets to see if there have been variable changes, to include possibilities of precipitation shortages or abundances. The data sets occur during the period of January 2005 through January 2017. Findings show a pattern between wind speed, precipitation and temperature. Results show the strong correlation between temperature variation and wind speed variation in reference to high and low pressure system changes as was suspected. I found no significant correlation between temperature change and precipitation. Only non-informative correlation between wind speed and precipitation was found in the high and low pressure system changes that precedes and during precipitation fall. I found no conclusive data to show that the precipitation had any direct effect on wind speed or vice versa. I compared these findings compared to studies conducted by Pryor et al., 2009. This study will be helpful in the future in predicting the wind speed and the future usage of renewable energies.

Keywords: climate, precipitation, wind, temperature

PDF malware detection with image processing and classification techniques

DONOVAN JENKINS, NEW MEXICO TECH

JUN ZHENG, NEW MEXICO TECH

ANDREW CORUM, CALVIN COLLEGE

PDF (Portable Document Format) is a file format invented by Adobe for presenting, exchanging and archiving document that is independent of hardware, software, and operating systems. PDF file has a flexible structure that can embed different kinds of contents such as JavaScript code, encoded streams, and image objects etc., which can be exploited by cybercriminals to embed malicious code using tools like Metasploit. In this project, we propose a new method to detect PDF malware using image processing and classification techniques. The PDF files are first converted to images using byte plot or Markov plot. Then various image features are extracted from the images that can represent the distinct visual characteristics of PDF malware and legitimate PDF files. Finally, machine learning algorithms are employed to build the classification models to predict a new PDF file as benign or malicious. We evaluated the performance of the proposed method using Contagio PDF malware dataset. The results show that our method can achieve a 99.48% F1 score which is better than that of many popular antivirus scanners such as Symantec, Microsoft, nProtect etc. It is also shown that the proposed method is more robust to resist reverse mimicry attacks than the state-of-art machine learning-based method.

Keywords: PDF malware, image processing, image features

Understanding the distribution of rain and snow during Atmospheric River events: A case study of the 1861-62 event

JONATHAN KANE, UNIVERSITY OF NEW MEXICO

LOUIS A. SCUDERI, UNIVERSITY OF NEW MEXICO

Atmospheric Rivers (AR) are narrow bands of water vapor transport, responsible for 90% of mid-latitude water transportation as well as intense and prolonged precipitation events. In the late 1861-1862 an AR event produced flooding that caused a magnitude of economic impacts. We hypothesize that precipitation from these events produces a change in the response of both high-altitude temperature sensitive trees and low-altitude precipitation sensitive trees and that these responses can be used to quantify this event. We created normalized growth indexes for each individual tree ring record and correlated the growth with factors such as altitude and species to quantify the growth.

Analysis of the mapped tree growth response is used to extract a coherent signal that may be representative of AR events in general. This signal could then be used to determine if similar extreme AR events occur in earlier portions of the tree ring record. Analysis of this dataset will allow us to better understand, monitor and predict the impact of large AR events on California. The frequency and strength of AR events impacts the length of droughts, intensity of floods, ecosystem response and ultimately impacts on humans.

Keywords: Atmospheric Rivers, climate, historical flooding

Developing a mental model

ISAIAH LILJESTRAND, NEW MEXICO TECH

A mental model is a useful tool for describing user's general mental processes that go into certain actions. In this paper, we investigate how to enhance the usability of security applications by considering human factors. Specifically, we study how to better understand and develop the user's mental model in the context of computer security through the use of the reasoned action approach (RAA). RAA explains that a user's behavior is determined by her intention to perform the behavior and the intention is, in turn, a function of attitudes towards the behavior, perceived norms (or social pressure), and perceived behavior control (capacity and relevant skills/abilities). A user study was conducted to test the validity of each of the main components of the model. Our user study concluded that alterations to a computer security application improved by the analysis through the mental model created improved user behavior.

Keywords: mental model, human behavior, user studies

Turbidity in the San Juan River and its association with arsenic and lead

MARIAH PAUL, DINÉ COLLEGE

PALOMA BEAMER, UNIVERSITY OF ARIZONA

NEILROY SINGER, DINÉ COLLEGE

YOSHIRA ORNELAS VAN HORNE, UNIVERSITY OF ARIZONA

PERRY CHARLEY, DINÉ COLLEGE

KARLETTA CHIEF, UNIVERSITY OF ARIZONA

JANI INGRAM, NORTHERN ARIZONA UNIVERSITY

On August 5th, 2015 the Gold King Mine Spill had accidentally released contaminated waste water which contained arsenic and lead. The spill began in the Animas River, eventually affecting the San Juan River which lead to Lake Powell. The Navajo Nation uses the San Juan River for irrigation, livestock, and ceremonial purposes. Dr. Karletta Chief's research team collected water samples from March through August 2018 at five locations along the river. The research team measured conductivity, turbidity, temperature, total dissolved solids, and ph. The water samples were collected and acidified to a pH of <2 using nitric acid, they were then shipped to NAU, Northern Arizona University, for analysis. Using an ICP-MS machine the lead and arsenic were measured, arsenic ranged from 0.06 to 0.085 ppb, and lead ranged from 0.018 to 0.023 ppb. While there is an association between turbidity and the concentration of arsenic and lead, it is not significant. Arsenic and lead concentrations were below the Navajo Nation EPA agricultural guidelines, 100 ppb and 5000 ppb, respectively. The Diné community always prays for clean water on the reservation. To them, water is life, it is medicine and most of all precious. Seeking information and bringing results to the community brings the Navajo community hope for clean water for their health, animals, and most of all land.

Keywords: water quality, arsenic, lead, inductively coupled plasma mass spectrometry (ICP-MS), turbidity

Characterizing vibration frequency sensitivity and neural activity in escaping earthworms*

ANDRES ROMERO, NORTHERN NEW MEXICO COLLEGE
WES COLGAN, NORTHERN NEW MEXICO COLLEGE

ULISES M. RICOY, NORTHERN NEW MEXICO COLLEGE

Escape responses are ubiquitous in the animal kingdom. There are over 6,000 known terrestrial earthworms, some of which have elaborate escape behaviors. In 2008, *Diplocardia mississippiensis* gained notoriety when multiple television crews reported on a southeastern traditional harvesting technique called "worm grunting". The leading theory for this behavior is predatory escape. Not all earthworms display this elaborate behavior, including *Lumbricus terrestris*, a species that is sold all over North America as live-bait; with reports of distribution of over 120 million worms annually from

one company alone. It can be deduced that there are streams and lakes all over the continent with non-native *L. terrestris* colonies. The specific earthworm escape behavior of *D. mississippiensis* is well documented and studied. However, there has been very little research into the neurobiology underlying these behaviors. We are interested in characterizing and comparing vibration sensitivity induced neural activity and behavior of the different worm species. Ethogram scoring and electrophysiological recording techniques were used. We designed an apparatus that can expose unrestrained worms to a range of frequencies. We also designed an apparatus that isolates the anterior end of the worm to maintain a secure suction electrode placement for extra cellular recordings from the subpharyngeal ganglion. We introduced the same discrete frequencies that induced notable behavior events and recorded the accompanied neural activity. With these protocols in place, we can investigate multiple species and better understand how these introduced worms may react to predation in new environments.

Keywords: earthworms, escape responses, vibration frequency

Increased chemo-sensitivity to DNA-damaging agents conferred by the exercise myokine, irisin in breast cancer cells

SHANIA VEL SANCHEZ, UNIVERSITY OF NEW MEXICO
RACHEL EARLEY, UNIVERSITY OF NEW MEXICO

HELEN HATHAWAY, UNIVERSITY OF NEW MEXICO

Breast cancer is a disease that affects 1 in 8 women. Epidemiological studies have shown that exercise is associated with a decreased risk of developing cancer, and improving prognosis of many cancer types, including breast cancer. Our studies demonstrate that irisin, a myokine produced by muscle cells upon exercise, increases the sensitivity of malignant p53 mutant MDA-MB231 breast cancer cells to the chemotherapeutic doxorubicin (dox) by over 90 fold. Irisin did not alter the dox sensitivity of malignant, p53 wild-type MCF7 breast cancer cells, or normal non-malignant MCF10A breast epithelial cells. Our studies will investigate the molecular mechanisms through which irisin sensitizes selected breast tumor cells to DNA damaging agents. Based on our data demonstrating that irisin induces chemo-sensitization only in the p53 mutant cells tested, we hypothesize that irisin sensitizes p53 mutant cells to DNA damaging chemotherapeutics by inhibiting cell cycle checkpoint genes, suggesting that irisin co-treatment may improve the effectiveness of current breast cancer therapeutics. Developing a dox/irisin combination therapy to achieve a significantly lower dox dosage would minimize the toxicities and side effects associated with DNA damaging chemotherapeutics. To identify the mechanism through which irisin is sensitizing cells, we are measuring proliferation, cytotoxicity, and apoptosis in the high throughput IncuCyte imaging system, in addition to metabolic endpoint assays. We will also assess the role of p53 mutations and downstream signaling pathways using knockdown and overexpression approaches. Our studies suggest that irisin may offer therapeutic benefits for breast cancer prevention and treatment.

Keywords: breast cancer, chemotherapy, biology, DNA

Plants in space: Interactions between morphology, lignification, and carbon isotopic composition

BIANCA SERDA, UNIVERSITY OF NEW MEXICO
MARGARET TURPIN, UNIVERSITY OF NEW MEXICO

PATRICK HUDSON, UNIVERSITY OF NEW MEXICO
DAVID HANSON, UNIVERSITY OF NEW MEXICO

Plants with the C3 photosynthetic pathway rely on diffusion of CO₂ from the atmosphere to the chloroplast to capture carbon for growth and development. Leaf anatomy, cell wall thickness, causes resistance to CO₂ diffusion with the heavier stable isotope of CO₂ (¹³CO₂) being slowed more than the lighter one (¹²CO₂). In addition, the CO₂ capturing enzyme in photosynthesis, Rubisco, uses ¹²CO₂ faster than ¹³CO₂. The net result of these anatomical and enzyme effects is that C3 plants capture more ¹²C when the resistance to diffusion is low, when cell walls are thin. Lignin is the part of cell walls that gives them rigidity and increases strength for withstanding gravity and mechanical forces. Therefore, it can affect how much plants invest making thick walls. We are growing a C3 species, *Arabidopsis thaliana*, with modifications to lignin content and photosynthesis, on the International Space Station (ISS) and Kennedy Space Center (KSC), in order to study how their growth and metabolism are affected under microgravity (space)

versus Earth's gravity. We hypothesize that the plants grown in space will have thinner cell walls, which will decrease resistance to CO₂ diffusion and decrease the ratio of ¹³C/¹²C in plant tissues. Our preliminary data on *Arabidopsis thaliana*, grown on Earth, demonstrates that our method for visualizing plant anatomy and lignin content works with frozen tissues, like those we will receive from the ISS. We are currently using this method to confirm relationships between the ¹³C/¹²C ratio, leaf anatomy, and lignin content on Earth-grown plants.

Keywords: photosynthesis, carbon dioxide, International Space Station

GRADUATE STUDENT POSTER ABSTRACTS

Poster session participants are listed alphabetically by last name of registered presenter. * indicates the poster received an outstanding Graduate poster award at the NMAS 2018 Research Symposium.

K-12 education component of sustainable bioeconomy for arid regions project

MESHACK AUDU, NEW MEXICO STATE UNIVERSITY

TRACIE MIKESSELL, MESILLA VALLEY LEADERSHIP ACADEMY

BRIAN TREFTZ, NEW MEXICO STATE UNIVERSITY

UMAKANTA JENA, NEW MEXICO STATE UNIVERSITY

CATHY BRADLEY, LYNN MIDDLE SCHOOL

CATHERINE BREWER, NEW MEXICO STATE UNIVERSITY

Sustainable Bioeconomy for Arid Regions (SBAR) is a USDA-funded 5-year coordinated agricultural project (CAP) begun in September 2017 to develop guayule and guar bioeconomies for the desert Southwest region of the U.S. SBAR is led by the University of Arizona (UA) and includes New Mexico State University, Colorado State University, Colorado School of Mines, Bridgestone Americas, and USDA ARS. As one of nine regional CAPs, SBAR includes research, education, extension and outreach components. Research thrusts for the project include feedstock development and production (crop breeding, agronomy, irrigation engineering), post-harvest logistics and co-products (harvest and transportation optimization, value-added co-products, biomass conversion to biofuels), and sustainability modeling (techno-economic analysis, life cycle assessment). Extension and outreach efforts include grower workshops and demonstration plots, extension publications, and 4-H youth camps and programs. With the development of hard rubber for tires, guar gum, animal feeds, chemicals, and biofuels from the two desert crops, there is a high potential for job creation. One goal of the SBAR education component is the development and implementation of STEM educational programs that will prepare the next generation of the labor force for those jobs. The SBAR Fellows program pairs graduate students doing research in SBAR-related fields with middle school science teachers to design and polish activities in formal classroom and informal settings. In summer 2018, six teacher-fellow pairs participated in a week-long 4-H biofuels camp hosted by UA, followed by a week of professional development to translate lessons learned in that camp for their classrooms in the 2018-2019 school year. The two New Mexico teacher-fellow pairs designed an afterschool STEM program called Guardians of the Biosphere to serve students at two middle schools in the Las Cruces Public Schools. Activities and demonstrations are built around the SBAR theme of guar and guayule for biofuels and bio-products, incorporating science, engineering and sustainability. Among the activities for the program are “dipping dots” liquid nitrogen ice cream, guar gum super-bubbles, conversion of vegetable oil into biodiesel, and creation of an aquaponics ecosystem for aquaculture and horticulture.

Keywords: Guar, guayule, sustainability, bio-economy, professional development

Bio-crude oil production from organic food waste

HENGAMEH BAYAT, NEW MEXICO STATE UNIVERSITY

JACOB USREY, NEW MEXICO STATE UNIVERSITY

NICHOLAS SOLIZ, NEW MEXICO STATE UNIVERSITY

CESAR MARTINEZ BEJARANO, NEW MEXICO STATE UNIVERSITY

FENG CHENG, NEW MEXICO STATE UNIVERSITY

CATHERINE BREWER, NEW MEXICO STATE UNIVERSITY

ALAN MOYA, NEW MEXICO STATE UNIVERSITY

UMAKANTA JENA, NEW MEXICO STATE UNIVERSITY

In recent decades, food waste has been one of the most serious social, economic and environmental problems. In 2010, the U.S. discarded approximately 30.8 million tons of organic fraction food waste (OFFW), accounting for 14% of total generated municipal solid waste. OFFW is an inexpensive, energy-dense alternative to edible crops and has the potential to be converted into liquid transportation fuels. Most OFFW has high moisture content and is composed of carbohydrates, proteins, and lipids. Hydrothermal liquefaction (HTL) is a promising conversion methods for high-moisture content materials because HTL requires no initial drying, unlike the other thermochemical processes such as gasification and pyrolysis. HTL involves pressure-cooking of organic constituents in hot compressed water and produces an energy-dense liquid fuel, called bio-crude oil. This research targets the viability of HTL for OFFW and the effect of operating conditions on bio-crude oil yield and quality. OFFW was collected from lunch leftovers from Taos (cafeteria style) Restaurant at New Mexico State University, and characterized for physical and chemical properties. HTL of OFFW was performed using a 100 ml batch reactor at 240-295 °C, 15% OFFW solids

loading, and 30 min. reaction time. Bio-crude oil yields ranged from 20-27% on a dry mass basis. HTL product characterization includes higher heating value, elemental composition, and chemical constituents. Preliminary findings suggest that HTL of OFFW can be effective for organic waste management and bioenergy production.

Keywords: organic food waste; hydrothermal liquefaction; bio-crude oil

Changing the way water boils on surfaces

LAZAR CVIJOVIC, NEW MEXICO STATE UNIVERSITY

Boiling of water to transfer heat has numerous applications, e.g., in power generation, water purification, and cooking. When water boils over a surface, substantial amounts of heat can be transferred from the surface to the water without causing a significant increase in the surface temperature; hence, boiling is also used in applications such as cooling of nuclear reactor rods and electronics where large temperature rises are prohibitive. However, when a large amount of heat must be removed from a small area through boiling, it encounters a crisis called the Critical Heat Flux (CHF) limit. At this limit, the rapidly generated vapor bubbles merge to form a vapor film on the hot surface which prevents liquid water to contact the surface. This project pursues a new type of surface, called the Binary Surface(s) (BiS), for extending the current CHF limits for the boiling of water. A BiS is a highly wetting surface with many sub-surface micro-/nano-cavities, which are filled with a Non-Boiling Liquid (NBL) creating puddles around solid islands. The goal of this research project is to experimentally measure the CHF and the Heat Transfer Coefficient for the pool boiling of water on a copper-oil BiS (oil is the NBL) and compare them with those obtained on plain surfaces. Details of the BiS surface preparation and the boiling heat transfer experiments on these surfaces will be presented. This research helps to establish the feasibility of a new boiling enhancement mechanism that could have a significant impact in many critical fields.

Keywords: boiling water, materials chemistry, surfaces

Bluetooth operation verification via monitoring the transmission pattern using machine learning

ABDELRAHMAN ELKANISHY, NEW MEXICO STATE UNIVERSITY

Bluetooth is a widely-used wireless communication protocol in small portable devices due to its low energy consumption and high transfer rates. Manufacturers normally buy their Bluetooth chips from third-party suppliers, which are then integrated into a complex hardware-software stack with a variety of potential vulnerabilities. Direct measurement of the output can help security functions prevent unauthorized data transmission. This work proposes a compact supervisory circuit to classify the operation of a Bluetooth chip at low frequencies by monitoring the radio frequency (RF) output of the Bluetooth chip through an envelope detector. The idea is that the envelope detector and classification algorithm can be inexpensively fabricated on a low-frequency integrated circuit in legacy technology and/or with minimal area. When the supervisory circuit detects abnormal behavior, it can be configured to shut down the Bluetooth chip. Using features extracted from the envelope of the RF output signal, we are able to train several machine learning (ML) algorithms to classify different Bluetooth operation modes and parameters such as operation profile, distance between the paired devices, and number of connected devices. In this work, we demonstrate ML models that can separate Bluetooth advertising and transmit/receive modes with ~100% accuracy and classify the operation profile of the Bluetooth chip with ~100% accuracy.

Keywords: Bluetooth, machine learning, security, RF signals, and supervisory circuit

Ray matrices and SpMV compression methods

*AMMAR ELWAZIR, NEW MEXICO STATE UNIVERSITY ABDEL-HAMEED BADAWY, NEW MEXICO STATE UNIVERSITY
DAVID VOELZ, NEW MEXICO STATE UNIVERSITY*

Ray tracing is an efficient way to determine the performance of an optical system. For the ray transfer matrix approach, all interfaces and optical components, such as mirrors, lenses and distances, are define by a 2x2 matrix known as the ABCD matrix. The ABCD matrix transfers the input ray parameters (height and angle) to new output

ray parameters and multiplying the component ABCD matrices gives the overall system matrix. However, complicated optical systems may have tens or hundreds of component matrices and hundreds of rays that need to be traced. Furthermore, the optimization of the system component parameters often takes many repetitions of the ray tracing process. Therefore, improving processing speed and reducing data storage is important. One solution is to use multiprocessor hardware, such as GPUs, to reduce the time for the matrix calculations but this solution can be expensive. In this work, we discuss an approach to improve the efficiency of the matrix multiplications. Most of the matrices for interfaces, mirrors, lenses or even distance contain zero values so we apply the coordinate format compression method to compress these matrices so zero values are excluded. The significant values are placed in a vector and their row and column indices are stored in two vectors. We split every row in the matrices to be multiplied in a single thread so it can work in parallel and the process time for all the multiplications is the just the time to multiply every row. In initial testing with systems involving several matrices and without the multithreading part, we found out that the process time is approximately 60% of the time required for conventional matrix multiplication. When multithreading is implemented, we are predicting the time to finish the multiplication will be equal to the time for the multiplication of only one row. For this work, we implemented a Graphical User Interface to test the compression approach and are currently considering how to combine the compression method with GPU systems.

Keywords: GPUs, ray matrices, optical systems, engineering

Joint source-channel coding with concatenated spatially coupled LDPC codes

AHMAD GOLMOHAMMADI, NEW MEXICO STATE UNIVERSITY

Joint source-channel coding (JSCC) involves the use of a single coding scheme in order to encode data from a redundant information source (source coding/data compression) for reliable transmission over a noisy channel (channel coding/error correction). JSCC can be attractive in the non-asymptotic regime, where the residual redundancy of the source sequence can be used by the channel decoder to improve channel decoding. In this work, a method for JSCC based on concatenated spatially coupled low-density parity-check (SC-LDPC) codes is investigated. A construction consisting of two SC-LDPC codes is proposed: one for source coding and the other for channel coding, with a joint belief propagation-based iterative message passing decoder. Using a windowed version of the decoder, simulation results show a notable performance improvement compared to existing state-of-the-art JSCC schemes based on LDPC codes for approximately equal latency and complexity requirements.

Keywords: joint source-channel coding, transmissions, engineering

I can fly if I wanted to: effectiveness of tip cross-sectional area versus perimeter in identifying potential lithic armatures

JACKSON GRADY, UNIVERSITY OF NEW MEXICO

Killing prey from a distance using complex projectile weapons is a behavior unique to *Homo sapiens*. The archeological remnants of these weapons are mostly limited to their lithic points, as their organic components have decomposed. In order to distinguish these points from stones fashioned for other purposes and more accurately determine the advent of this advanced technology, researchers have primarily utilized a measurement known as tip cross-sectional area (TCSA). This metric was thought to be the most ballistically significant one available for this purpose based on studies of high velocity projectiles. Sisk and Shea (2011) hypothesized that tip cross-sectional perimeter (TCSP) is a more useful ballistic measurement when identifying low velocity projectiles such as arrows and darts. To test this idea, we designed and printed six arrowheads divided into pairs with either the same TCSA but different TCSP, or the same TCSP but different TCSA. Our results support the Sisk and Shea hypothesis that TCSP is a better predictor of a point's penetration than TCSA. We also found that surface area, which is highly correlated to TCSP, may be the most useful ballistic measurement for low velocity projectiles. Utilizing TCSP and surface area, rather than TCSA, may allow archeologists and anthropologists to more accurately categorize points found in archeological sites prior

to 40ka, a watershed moment in the development of modern human behaviors and population growth. If projectile weapons are identified prior to 40ka, their development may have served as a catalyst in the early cognitive evolution of man.

Keywords: archeology, population growth, human behavior, lithic armatures

Mineralogy controlled dissolution of uranium from airborne dust in simulated lung fluids (SLFs) and possible health implications

ESHANI HETTIARACHCHI, NEW MEXICO TECH

BONNIE FREY, NM BUREAU OF GEOLOGY

SHAYLENE PAUL, NAVAJO TECHNICAL UNIVERSITY

GAYAN RUBASINGHEGE, NEW MEXICO TECH

DANIEL CADOL, NEW MEXICO TECH

The recent increase in cardiovascular and metabolic disease in the Navajo population residing close to the Grants Mining District (GMD) in New Mexico is suggested to be due to exposure to environmental contaminants, in particular uranium in respirable dusts (fine dust small enough to reach gas exchanging/ alveolar region of lungs). However, the chemistry of uranium-containing-dust dissolution in lung fluids and the role of mineralogy are poorly understood, as is their impact on toxic effects. The current study is focused on the dissolution of respirable-sized U-containing-dust, collected from several sites near Jackpile and St. Anthony mines in the GMD, in two simulated lung fluids (SLFs): Gambel's solution (GS) and Artificial Lysosomal Fluid (ALF). We observe that the respirable dust includes uranium minerals that yield the uranyl cation, UO_2^{2+} , as the primary dissolved species in these fluids. Dust rich with minerals uraninite and carnotite is more soluble in GS, which mimics interstitial conditions of the lungs. In contrast, dust with low uraninite and high kaolinite is more soluble in ALF, which simulates the alveolar macrophage environment during phagocytosis. Moreover, geochemical modeling, performed using PHREEQC, is in good agreement with our experimental results. Thus, the current study highlights the importance of site-specific toxicological assessments across mining districts with the focus on their mineralogical differences.

Keywords: uranium, lung fluids, heavy metal inhalation

Identifying and controlling the impacts of mining activities on groundwater quality in the state of New Mexico

STACY KUYKENDALL, UNIVERSITY OF NEW MEXICO

PEDRAM ROGHANCI, UNIVERSITY OF NEW MEXICO

Groundwater pollution poses a serious threat to both human health and to ecosystem stability. Sources of groundwater impacts from mining activities require identification to better develop solutions to protect. This research will identify solutions to this problem, while also raising awareness of the impact of abandoned mines on groundwater contamination. Abandoned mines in New Mexico are often unmonitored, and little data is available as to their effect on groundwater quality. Solutions to impacts that abandoned mines have on groundwater quality will be recommended by determining monitoring procedures and cost-effective cleanup plans based upon the level of groundwater contamination. Both the mining industry and regulatory agencies need to employ advanced treatment techniques to protect groundwater from the influence of closed and abandoned mines to minimize environmental impacts. This research will develop strategies to minimize that disturbance both to the groundwater and to the surrounding habitat. It is evident that continued environmental stewardship and a focus on future cleanup plans and ongoing mine site restoration should be a part of every mine's operating process.

Keywords: groundwater; mining activities; abandoned mines; treatment techniques; remediation

Synthesis of novel ladder-type oligo p-phenylenes for use in organic solar cells*

VANCE MILLER, EASTERN NEW MEXICO UNIVERSITY

The development of phenylene and fluorene based compounds has the potential to yield low-cost, readily available, semiconductor materials that can be used in a wide range of applications involving organic electronics. This study aims to synthesize specifically tuned nitrile-substituted ladder-type oligo-p-phenylenes to be later characterized and

evaluated for applications in organic photovoltaics. These compounds have the potential to meet the charge carrier mobility, structural stability, affordability and ease of manufacture that is essential for large scale production components of the active layers in organic photovoltaics. The expected synthetic route for the target compounds follows a multi-step process involving multiple Suzuki cross-coupling, cyclization, alkylation, bromination, and lastly nitrile substitution reactions. Future instrumental assessments should reveal whether or not this material meets the criteria for use in the active layers of organic photovoltaics, specifically as an n-type semiconductor.

Keywords: semiconductors, organic photovoltaics, chemistry

Accurate positioning of quadrotor UAVs using a Wii remote camera and signal modulations for outdoor precision landing

BRIAN MOLLEY, NEW MEXICO TECH

KOOKTAE LEE, NEW MEXICO TECH

Over a few decades, rapid advances in micro-controller and sensor technologies have brought proliferation of quadrotor Unmanned Aerial Vehicles (UAVs). This type of UAVs has been widely used in a variety of fields including monitoring and inspection, surveillance, search and rescue, military, and drone delivery. In these missions, an autonomous flight feature becomes increasingly important and popular as it can provide autonomy of quadrotor UAVs during missions with more accuracy without human intervention. Unlike the autonomous flight stage, where the position is provided by GPS, the autonomous landing requires higher accuracy as collisions that may occur during the landing stage can cause severe damages. Although many research works have contributed to the development of precision landing, they either require expensive platforms or have been developed for indoor use. In this research, we develop a low-cost quadrotor platform for outdoor precision landing using Wii remote camera and Infra Red (IR) beacons. As this camera is sensitive to the sunlight that contains broad spectrums of IR light waves, the reflection of sunlight from environments may disturb the accurate positioning of a quadrotor. To circumvent this issue, we implement a signal modulation technique in which the IR beacons from the ground station transmit a modulated signal to the camera. If the camera receives this modulated signal with fixed pattern, the quadrotor recognizes this light source and hence, differentiates it from sunlight disturbances. This method will significantly contribute to the outdoor UAV precision landing in a cost-efficient manner.

Keywords: UAV, precision landing, signal modulation

The effect of transcranial direct current stimulation (tDCS) on audition

AUDREY MORROW, NEW MEXICO STATE UNIVERSITY

MICHAEL HOUT, NEW MEXICO STATE UNIVERSITY

AMIE AMIOTTE, NEW MEXICO STATE UNIVERSITY

JUSTIN MACDONALD, NEW MEXICO STATE UNIVERSITY

Individuals can experience hearing impairments from both structural and functional changes. Several auditory processing functions have shown to be enhanced with transcranial direct current stimulation (tDCS) in normal hearing individuals, such as improved syllable identification and language learning when applied to language areas. However, there is limited research aimed at using tDCS to improve individual hearing abilities in a way that could benefit those who experience hearing difficulties. This study used two experiments to identify whether there were changes in speech perception or tone detection in normal hearing individuals when anodal tDCS was applied to auditory areas of the brain. Experiment 1 bilaterally stimulated the primary auditory cortices (T3 and T4) for 10 minutes each, counterbalanced. These areas are contained in the superior temporal gyrus and mediate our ability to hear and process auditory input. Experiment 2 stimulated the left posterior superior temporal gyrus (halfway between T3 and T5) for 20 minutes, an area which contains Wernicke's and Broca's areas and is heavily involved in processing sounds. In both studies, we used a sham stimulation setting for the control group. There were no significant differences between stimulation and sham condition in either experiment for either task. These results suggest that this level of audition may be reliant upon structural components rather than functional or auditory processing changes.

Keywords: transcranial direct current stimulation (tDCS), audition, auditory cortex, superior temporal gyrus

Wastewater remediation and indoor cultivation of algae for biodiesel production

JAYAMINI MUDUGAMUWA HEWAGE, EASTERN NEW MEXICO UNIVERSITY

Microalgae has been used in research for biodiesel production for many years. The reason for choosing microalgae rather than other lipid containing sources is because algae takes up carbon dioxide, a greenhouse gas and can be cultivated in any harsh condition. In addition to being used as a possible biofuel source, algae is also being used as a potential food source for humans and animals, a major ingredient in the cosmetic and pharmaceutical industries. Currently another issue that the world faces is disposing of dairy and agricultural wastewater. This research is based on cultivating algae in untreated dairy wastewater. This wastewater comes from a local Portales dairy near the university and it contains nutrients which facilitate the growth of algae. Using indoor cultivation in a photobioreactor, giving artificial light conditions, the growth of algae in wastewater is monitored to maximize biomass productivity. The growth rate and biomass concentration are obtained from UV-vis spectroscopy by determining the optical density values at a specific wavelength. The dairy wastewater is not directly applied for the growth, but standard medium is used to dilute it to a usable range. Procedures are followed to make the wastewater suitable for the cultivation of algae. The wastewater before and after cultivation is examined to obtain the nutrient uptake of algae for nitrogen and phosphorus. The lipid in dry algae is extracted using Soxhlet extraction. The percentage lipid content in indoor and outdoor cultivation is compared, also the different fatty acids found in both cultivations are determined using GC-MS technique.

Keywords: microalgae, biodiesel, GC-MS, indoor cultivation

Lead selenide quantum dots for use in solid-state radiation detectors

TOM NAKOTTE, NEW MEXICO STATE UNIVERSITY
HONGMEI LUO, NEW MEXICO STATE UNIVERSITY

JEFFERY PIETRYGA, LOS ALAMOS NATIONAL LABORATORY

The unique optical and electrical properties of lead selenide (PbSe) quantum dots (QDs); which are due to quantum confinement effects that are a product of their nanometer scale sizes, have made PbSe QDs an interesting material for various devices from solar cells to photodetectors. Here we aim to leverage another important property, the high Z number of the material, to fabricate solid-state radiation detectors for high energy waves such as x-rays and gamma-rays. PbSe QDs are prepared using colloidal synthesis techniques which employ a weakly binding oleylamine ligand as the stabilizing ligand, for the purpose of fabricating a solid-state radiation detector using PbSe QDs as both the blocking and detection layers. Using oleylamine rather than the more traditional strongly binding oleate ligand allows for the facile in-solution ligand exchange with shorter anionic ligands. QDs passivated with shorter ligands are then implemented into testing devices (such as FETs, capacitors, and simple photodetectors) by spin-coating the colloidal solution into films. Thicker films, which are necessary for attenuation of x-rays and gamma-rays, can be fabricated by using more concentrated solutions and slower spin speeds; without the need for additional layer-by-layer ligand exchange steps, which has hampered and prolonged the fabrication time of thick QD films in the past. Data collected from research devices, such as carrier mobility and carrier capacity, is then used to calculate the performance and assess the feasibility of PbSe QDs as a material for use in low-cost solution processed solid-state radiation detectors.

Keywords: colloidal synthesis, PbSe, quantum dots, radiation detection

Twenty years of herping: updated visual representation of species richness

VINICIUS ORTEGA-BERNO, EASTERN NEW MEXICO UNIVERSITY
WILLIAM PARISH, EASTERN NEW MEXICO UNIVERSITY

IVANA MALI, EASTERN NEW MEXICO UNIVERSITY

Based on herpetofaunal records, New Mexico is one of the most diverse states in the American Southwest. We visually summarized reptile and amphibian diversity in New Mexico using occurrence data from the past 20 years. We also identified patterns of species richness by county and discuss survey bias as a factor. In general, northwestern counties had the lowest number of species while central and southwestern regions had the highest numbers of species. We also recognized species-rich counties with few to no new county records in the past 20 years as areas that potentially reached survey saturation.

Keywords: herpetofauna, richness, New Mexico

Attentional sensitivity and behavioral modeling of social grooming among immature East African chimpanzees (*Pan troglodytes schweinfurthii*) of the Kanyawara community at Kibale National Park*

KRISTIN SABBI, UNIVERSITY OF NEW MEXICO

ZARIN MACHANDA, TUFTS UNIVERSITY

MELISSA EMERY THOMPSON, UNIVERSITY OF NEW MEXICO

EMILY OTALI, KIBALE CHIMPANZEE PROJECT

MARTIN MULLER, UNIVERSITY OF NEW MEXICO

RICHARD WRANGHAM, HARVARD UNIVERSITY

Recent developmental studies of wild chimpanzees (*Pan troglodytes schweinfurthii*) at Gombe argue that sex differences in adult sociality may be rooted in mothers adjusting their social strategies when they have sons versus daughters. Though early life social experience has important effects on social behavior later life, underlying sex differences in attention to and modeling of social interactions could exacerbate differential social exposure to encourage diverging social strategies during development. If so, adult social patterns should be reflected in immatures' attentional sensitivity to social interactions. Since adult male chimpanzees groom peers more often than females, young males should spend more time watching neighbors' grooming bouts and be more likely than females to begin grooming bouts immediately following exposure. To test this, we video-recorded chimpanzees under 10 y.o. at Kanyawara (n=24) in Kibale National Park, Uganda, for two minutes immediately following the start of grooming bouts between their nearest neighbors. We then scored the amount of time that immatures spent watching (TSW) grooming bouts and whether that immature groomed a partner after watching. TSW increased with age (GLMM, Int=23.61, $\beta_{\text{age}}=1.998$, $p=0.01$) but there was no sex difference in TSW ($p=0.39$). However, males were inherently more likely begin grooming a partner immediately following exposure (logistic regression, Int=-3.39, $p<0.01$; $\beta_{\text{sex}}=4.09$, $p=0.03$) and, further, males that watched longer were especially likely to begin grooming ($\beta_{\text{sex*tsw}}=0.08$, $p=0.03$). This supports the conclusion that underlying differences in attentional sensitivity may amplify the effects of differential exposure to shape the development of sex-typed social strategies in wild chimpanzees. This project supported by the Wenner-Gren Foundation, Nacey P. Maggioncalda Foundation, American Philosophical Society, and the Leakey Foundation.

Keywords: wild chimpanzes, behavior modeling, social grooming, Uganda

Chemical variations among particle size fractions: examples from uranium deposits in New Mexico

MARCUS SILVA, NEW MEXICO TECH

JOHN ASAFO-AKOWUAH, NEW MEXICO TECH

VIRGINIA MCLEMORE, NM BUREAU OF GEOLOGY

BONNIE FREY, NM BUREAU OF GEOLOGY

Weathering of minerals involves surface reactions, and the rates of these reactions depend upon the available reactive surface area of the minerals. Mineral surface area is dependent on the mineralogy, chemistry, the extent to which the mineral is liberated from the rock matrix, particle size, and the surface morphology. Prior studies of metal deposits indicate that weathering is more pronounced in the fine-size fraction than in the coarse-size fraction, an observation consistent with the increase of surface area with decreasing particle size. Studies of chemical variations among particle size fractions can be used to 1) understand weathering of mine waste, 2) determine the best size fractions for prediction tests, such as humidity cell or other leach tests, 3) help plan and assess reclamation procedures, 4) understand the mobility of elements of concern, and 5) provide background data that can assist with the planning of future mining operations. Four composite samples, sieved in the field to less than 12.5 mm, were collected from waste rock piles at two inactive uranium mines in New Mexico and analyzed for major and trace elements. These samples were further sieved into six size fractions. The samples are heterogeneous and range in concentration from 24 to 11,050 ppm U. Chemical analyses indicate that U is correlated ($R>0.6$) with V, LOI, C, Zr, Y, Pb, As, Se, and heavy REE. U, As, and C decreased in concentration with increase in particle size in the Jeter sample. However, U increased with increasing particle size or was concentrated in the middle sizes in the St. Anthony samples, whereas As and C had complex variations with change in grain size. These results suggest that weathering of certain U deposits may be more complex than previously thought and that this is largely tied to the organic material that hosts the uranium. However, more research is needed.

Keywords: uranium, mineral weathering, particle transport, legacy mines

Feasibility of using computer-assisted software for recognizing individual Rio Grande Cooter (*Pseudemys gorzugi*)*

THANCHIRA SURIYAMONGKOL, EASTERN NM UNIVERSITY IVANA MALI, EASTERN NEW MEXICO UNIVERSITY

Mark-recapture methods used in population demography studies involve marking of animals, such as tagging, notching, and tattooing. These techniques are invasive and potentially harmful to the animals. Photo-identification using natural animal markings is less invasive and has become more widely used for a range of taxa including invertebrates, fishes, reptiles, amphibians, and mammals. During 2016 and 2017, we studied the demographics of the Rio Grande cooter (*Pseudemys gorzugi*) using traditional mark-recapture techniques (i.e., shell notching and toe clipping). However, *P. gorzugi* displays plastral marks that could potentially be used for individual recognition. Because the photo-identification process 'by-eye' is time consuming, we tested the efficiency of three pieces of software: I3S Pattern+, Wild.ID, and APHIS, for individual identification of *P. gorzugi* using plastron pattern. Matching results of each program were generated into ranks with the 1st rank being the most likely match. Within the top 20 ranked images, Wild.ID yielded the highest number of correct matches (83.87%), followed by APHIS (ITM; 69.35%), APHIS (SPM; 67.74%), and I3S Pattern+ (61.29%). We found the quality of photos significantly contributed to the software effectiveness, however turtle age and plastron wear did not affect the accuracy of the photo-identification software. We concluded that Wild.ID can be used as a non-invasive photo-recognition technique for *P. gorzugi* in a short-term population study.

Keywords: photo-id, wildlife, turtle, conservation

Heat management in underground mines: personal risk factors, mitigation practices, and industry actions

ELAHEH TALEBI, NEW MEXICO TECH

PEDRAM ROGHANCI, NEW MEXICO TECH

There are many mining hazards that have long-term effects on the health, safety, and the life quality of mine workers. Some of these effects can be diagnosed immediately, others manifest after a period of time. Heat is a hazard that may be underestimated in many mining operations because people are unaware of its effects due to a lack of education in salient consequences of heat exposure. Hot and humid environments can negatively impact the health, performance, overall productivity, and the ability of the underground workforce to perform their job safely. The human body's reaction to excessive heat stress is different from person to person predominantly because the individual response to heat exposure is related to the each person's state of health and personal risk factors. Therefore, it is crucial to implement a heat management protocol to minimize the negative effects of heat exposure in underground mines. This project aims to promote heat management to control heat exposure and reduce heat-related incidents in the mining industry three levels; the individual level, corporate level, and industrial level. For each level, climatic heat stress risks, mitigation practices, and prevention methods are discussed. Furthermore, steps needed to implement the best heat exposure controlling techniques are addressed. We hope to find significant data that leads to policy recommendations to improve working conditions in underground mines.

Keywords: heat exposure, heat stress, heat-related incidents, mitigation practices

Size effect of gold nanoparticles on graphene quantum dots' fluorescence intensity

YUWEI ZHANG, NEW MEXICO HIGHLANDS UNIVERSITY

JIAO CHEN, NEW MEXICO HIGHLANDS UNIVERSITY

ZACK SCHROER, NEW MEXICO HIGHLANDS UNIVERSITY

Graphene quantum dot (GQD) is a new type of nanomaterials, which has gained great attention in many application fields, such as biological, optoelectronic, and energy-related fields. They have some unique properties, such as strong and stable fluorescence emission, good chemical inertness, outstanding biocompatibility, low toxicity, and low-cost preparation; Therefore, they have been applied in various biosensors as "fluorophores" Gold nanoparticles (AuNPs) are good quenchers to many organic fluorophores as well as GQDs. However, very limited studies have been focused on the mechanism of the AuNPs quenching on GQDs. This study will broaden the application fields of GQDs, especially in bioanalytical field and biosensor design.

Keywords: quantum dots, fluorescence, chemistry

FACULTY POSTER ABSTRACTS

Poster session participants are listed alphabetically by last name of registered presenter.

Detection and verification of periodontal pathogens through real time PCR

NIKITA DOUGAN, UNIVERSITY OF NEW MEXICO

ARJUN SENTHIL, UNIVERSITY OF NEW MEXICO

NATHAN WITHERS, UNIVERSITY OF NEW MEXICO

DEYANAHH WALKER, UNIVERSITY OF NEW MEXICO

JANE NGUYEN, UNIVERSITY OF NEW MEXICO

MAREK OSINSKI, UNIVERSITY OF NEW MEXICO

The detection and verification of *Streptococcus gordonii*, *Fusobacterium nucleatum*, and other oral bacteria is crucial to scientific research involving periodontal diseases and can be done using a Quantitative Polymerase Chain Reaction (Q-PCR) experiment. Experimentation using Q-PCR provides fast and accurate bacterial strain detection over a span of two to six hours [1] compared to traditional microbiology techniques which may take up to 48 hours or more.

This research project focuses on the detection and quantification of *S. gordonii*, *F. nucleatum*, and compound biofilms of both bacteria before and after the application of an experimental antimicrobial agent. The quantification of these bacteria through Q-PCR is important in detecting contamination of the experimental samples and in verifying the specific species of bacteria present in a sample. In order to confirm that the bacteria cultures have not been contaminated, a Q-PCR thermal cycler will be used for accurate testing conditions and analyses. Two gene-specific primers for both bacteria are required to amplify the bacteria to a detectable level. Results of the Q-PCR experiments will be determined through the analysis of the graph produced by the StepOnePlus Q-PCR machine and electrophoresis of the samples. Samples that are successfully amplified and confirmed to be either *S. gordonii* and/or *F. nucleatum* are expected to fluoresce and be detected during the reaction. Samples of bacteria, following verification through Q-PCR and electrophoresis, will be used for testing in further research in developing antimicrobial oral products.

Keywords: Q-PCR, PCR, primer, DNA template, *S. gordonii*, *F. Nucleatum*, quencher, reporter dye

Nanotechnology using iridium, platinum and osmium clusters

AJIT HIRA, NORTHERN NEW MEXICO COLLEGE

We continue our interest in the clusters of metallic elements in this investigation of the physical and chemical properties of Ir_m, Pt_m, and Os_m clusters, ($1 \leq m \leq 6$, $1 \leq n \leq 6$) and their hybrids with O₂, CO and CO₂. Platinum-group metals (abbreviated as the PGMs) which are also called, the platinoids, platinides, platidises, platinum group, platinum metals, platinum family or platinum-group elements (PGEs), are six noble, precious metallic elements are found located together in the periodic table. These elements are all transition metals in the d-block (groups 8, 9, and 10, periods 5 and 6). The six platinum-group metals are ruthenium, rhodium, palladium, osmium, iridium, and platinum. They have similar physical and chemical properties, and are usually found in the same mineral deposits. Further subdivision is the iridium-group platinum-group elements (IPGEs) and the palladium-group platinum-group elements (PPGEs). We have used the hybrid ab-initio methods of quantum chemistry, particularly the DFT-B3LYP model, and the Many Body Perturbation Theory (MBPT)/MP2 model, to derive the optimal geometries for the clusters of interest. We compare the calculated binding energies, bond-lengths, ionization potentials, electron affinities and HOMO-LUMO gaps for the various clusters. Of particular interest to us are the structures based on IrO, PtO, OsO, IrO₂, PtO₂, and OsO₂, in the solid phase, and the structures IrO₃, PtO₂, OsO₃, and OsO₄ in the gas phases. For the very small clusters, C_{2v}, C_{4v} and D_{2v} symmetries dominate. Our results reveal many abrupt changes in structure and spectroscopy, as a cluster is built up from its constituents. The values of HOMO-LUMO gap are expected to decrease as the cluster size increases. We also investigate the effects of crystal symmetries corresponding to the bulk structures. In addition we discuss the possible stabilities of the various oxides at the platinum metal surfaces.

Keywords: nanotechnology, metals, materials science

Effects of different heights and stem diameters on survival rates of Jujube Suckers transplanted in a semi-arid farm in Portales

ZHIMING LIU, EASTERN NEW MEXICO UNIVERSITY

SANJIB SAPKOTA, EASTERN NEW MEXICO UNIVERSITY

Jujube (*Ziziphus jujuba*) belongs to family Rhamnaceae and its fruit is rich in nutrients. Although jujube fruit consumption is widespread in Asian countries it is relatively unknown to North America. Jujube tree is drought- and frost-tolerant and can be widely planted across the state of New Mexico. Recently, interest in jujube from consumers and growers is surging. The New Mexico Department of Agriculture has identified jujube as an alternative crop. The major challenge is a very limited availability of jujube trees. The objective of this project was to study the effects of heights and stem diameters on survival rates of jujube suckers transplanted in a semi-arid farm in Portales, Roosevelt County, New Mexico. A total of 72 suckers were planted in October of 2017. The heights of the suckers were less than 50, 50–100, 100–150 and above 150 cm. The stem diameters of the suckers were 0.015–0.24 cm. Observations on the suckers after one year transplantation demonstrated that the suckers with 50–100 cm height and 0.03–0.07 cm stem diameter had the highest survival rate. This result is useful for growers for planting jujubes in the semi-arid regions like New Mexico. It is expected that jujubes will become a valuable alternative fruit crop in the United States.

Keywords: Jujube, sucker height, stem diameter, survival rates

About the New Mexico Academy of Science

The New Mexico Academy of Science was founded in 1902 to foster scientific research and scientific cooperation, to increase public awareness of the role of science in human progress and welfare, and to promote science education in New Mexico.

Membership in the Academy is open to anyone interested in science, science education, or the other goals and programs of the Academy. Individuals engaged in scientific research or teaching at all levels are particularly encouraged to become members. Applications for membership as well as more information about the Academy and its programs can be found at <http://www.nmas.org>.

CONTACT INFORMATION

The New Mexico Academy of Science
c/o The New Mexico Museum of Natural History and Science
1801 Mountain Road NW
Albuquerque, New Mexico 87104
nmas@nmas.org
<http://www.nmas.org>

OFFICERS AND EXECUTIVE BOARD 2018

OFFICERS

President: Dr. John Emerson
President-Elect: Dr. Stephen Jett
Vice-President: Dr. Nancy Hurtado-Ziola
Treasurer: Michael Gonzales
Secretary: Malva Knoll
Past President: Dr. David Peters

DIRECTORS

Jayne C. Aubele, NMAS Teacher Awards Program & NMAS Lecture Series
Lynn Brandvold, New Mexico Junior Academy of Science & AAAS Delegate
Dr. Richard Nygren, National Youth Science Camp
Natalie Rogers, Editor, *Journal of Science*
Dr. Hartono Sumali, Community Relations
Dr. Shanalyn Kemme, Director at Large
Amalia Parra, Director at Large
Moyo Peterson, UNM Liaison

DIRECTORS EMERITUS

David Duggan
Dr. David Hsi
Harry Pomeroy (NMAS Fellow)
Mona Pomeroy
Dr. Maureen Romine



© NMAS 2018. All rights reserved

This is a publication by the New Mexico Academy of Science. NMAS does not discriminate on the basis of race, creed, color, national or ethnic origin, sex, physical disability, or sexual orientation.